MOMENTUM AND HEAT TRANSFER OF NON-NEWTONIAN FLUIDS AROUND A SQUARE CYLINDER UNDER THE INFLUENCE OF AIDING BUOYANCY

A DISSERTATION

Submitted in partial fulfillment of the

requirements for the award of the degree

of

Master of Technology

in

Chemical Engineering

(With Specialization in Computer Aided Process Plant Design)

By

SHISHIR GUPTA

DEPARTMENT OF CHEMICAL ENGINEERING

INDIAN INSTITUTE OF TECHNOLOGY, ROORKEE

ROORKEE-247667 (INDIA)

JUNE 2013

Declaration

I hereby declare that the work presented in this dissertation entitled "**Momentum and Heat transfer of non-Newtonian fluids around a Square Cylinder under the influence of Aiding buoyancy**" submitted towards partial fulfillment for the award of the degree of M.Tech. in Chemical Engineering with specialization in Computer Aided Process Plant Design at the Indian Institute of Technology, Roorkee is an authentic record of my original work carried out under the guidance of **Dr. A.K. Dhiman** (IIT Roorkee). I have not submitted the matter embodied in this dissertation for the award of any other degree.

Place:- Roorkee Shishir Gupta

Date:- Enrol. No.-11514022

Certificate

This is to certify that Mr. Shishir Gupta (Enrol. No.11514022) has completed the dissertation entitled **"Momentum and Heat transfer of non-Newtonian fluids around a Square Cylinder under the influence of Aiding buoyancy"** under my supervision.

(**Dr. A.K. Dhiman**)
Assistant Professor
Dept. of Chemical Engineering
IIT Roorkee

Acknowledgements

I would like to express my sincere gratitude to my supervisor, Dr. A.K. Dhiman for his encouragement, guidance and support. I would also like to thank Dr. V.K. Agarwal (Head of the Department) for providing me with the opportunity and the resources for my dissertation work. I would also like to extend my heartiest gratitude to all my lab mates, Ms. Vandana Gautam, Mr. Ritwik Ghosh, Mr. Alex Denial, Mr. Ram Pravesh and Mr. Deepak Kumar Dwivedi for helping me at every step of my project work. Finally, I would like to thank all the teaching and non-teaching staff of Chemical Engineering Department for making my two years of M.Tech, a truly enriching educational experience. Finally but not the least, I would like to thank to my parents and my family and the God for their support and blessings.

Shishir Gupta
11514022
M.Tech.(C.A.P.P.D.)

Table of Contents

List of Figures

List of Tables

Abstract

Mixed convection flow and heat transfer characteristics of non-Newtonian fluid flowing around a long square cylinder under the influence of aiding buoyancy are investigated in the vertical unconfined configuration for the Reynolds number (Re) = 75 - 150, power-law index (n) = 0.2 - 1 and Richardson number (Ri) = 0 - 1 for a constant Prandtl number (Pr) = 50. The values of both Drag coefficient and Nusselt number increase with Richardson number. Drag coefficient is observed to decrease with increase in Reynolds number but Nusselt number shows an opposite behavior i.e. it increases with Reynolds number. In the present range of conditions, the flow of shear-thinning fluids is truly pseudo-periodic in nature at high Reynolds numbers and/or at small values of power-law index (highly shear-thinning fluids).

Keywords

Square cylinder, Aiding buoyancy, Streamline, Isotherm, Drag, Nusselt number, power-law index

Nomenclature

C_p Specific heat of the fluid, J/kg K

C_D Total drag coefficient $\left(= \frac{F_D}{\frac{\rho U_\infty^2 D}{2}} \right)$

C_{DF} Friction drag coefficient $\left(= \frac{F_{DF}}{\frac{\rho U_\infty^2 D}{2}} \right)$

C_{DP} Pressure drag coefficient $\left(= \frac{F_{DP}}{\frac{\rho U_\infty^2 D}{2}} \right)$

CV Control volume

D Side of a square cylinder, m

F_D Total drag force per unit length of the cylinder, N/m

F_{DF} Frictional component of total drag force per unit length of cylinder, N/m

F_{DP} Pressure component of total drag force per unit length of cylinder, N/m

g Gravitational acceleration, m/s^2

Gr Grashof number $\left(= \frac{g\beta_v (T_w - T_\infty) D^3 \rho^2}{m^2} \left(\frac{U_{avg}}{D} \right)^{2(1-n)} \right)$

h Local surface heat transfer coefficient, W/m^2 K

H Width of the domain, m

I_2 Second variant of the rate of strain tensor, s^{-2}

k Thermal conductivity of the fluid, W/m K

m Consistency index

N_p Number of points

Nu_{avg} Nusselt number $\left(= \frac{\bar{h}D}{k} \right)$

n power-law index

Pr Prandtl number $\left(= \frac{C_p m}{k} \left(\frac{U_{avg}}{D} \right) \right)$

Re Reynolds number $\left(= \frac{\rho U_{avg}^{2-n} D^n}{m} \right)$

Ri Richardson number $\left(= \frac{Gr}{Re^2} \right)$

t Time, s

T Temperature, K

T_∞ Free stream temperature, K

T_w Temperature of the surface of the cylinder, K

U_∞ Uniform fluid velocity at inlet, m/s

U_{avg} Average velocity of fluid, m/s

U_x Component of the velocity in *x* direction

U_y Component of the velocity in *y* direction

X_d Downstream distance, m

X_u Upstream distance, m

Greek Symbols

¶ Rate of deformation tensor, s^{-1}

β Coefficient of volumetric expansion, K^{-1}

° Density of the fluid, kg/m^3

η Dynamic viscosity of the fluid, Pa.s

± Stress tensor

Subscripts

∞ Inlet condition

w Surface of the cylinder

CHAPTER - 1

INTRODUCTION

Non-Newtonian fluids are found to be industrially significant; hence researchers have tried to elucidate the role of non-Newtonian character of fluids heat transfer phenomena for obstacles of different shapes flooded in the flowing fluids. The impact of non-newtonian behavior on momentum transfer is also a subject of research. Nearly all commonly found non-Newtonian fluids such as polymer in fused state, pulp and paper suspensions or industrially viable systems (such as colloids and foams) show evidence of non-Newtonian characteristics displaying either pseudo-plastic or dilatant behavior in nature or time-dependence, etc. These materials are generally found to be processed under laminar flow conditions owing to the fact of their high viscosity.

1.1 Newtonian and non-Newtonian Fluids

1.1.1 Newtonian fluids:

Newtonian fluids are those fluids which follow the viscosity law of Newton which states that the shear stress acting on the surface of flowing fluids is directly proportional to the negative of velocity gradient. The viscosity law by Newton is given by

$$\tau = \mu\left(\frac{dv}{dy}\right)$$

Where τ = shear stress

μ = viscosity of fluid

$\left(\frac{dv}{dy}\right)$ = negative of velocity gradient

Every gas and the majority of liquids that have simple molecular structure and low molecular mass are normally falls in the Newtonian fluids category. The most common example of Newtonian fluids are water, benzene etc.

1.1.2 Non-Newtonian fluids:

Fluids that do not follow a linear relationship of stress and strain are known as non-Newtonian fluids. Usually these are intricate mixtures such as liquid solution of polymers. A Power-law or non-Newtonian fluid, is a normal Newtonian fluid with the relationship for shear stress, τ denoted as

$$\tau = k\left[\frac{\partial v}{\partial y}\right]^n$$

Where τ = shear stress

k = non-Newtonian consistency index

n = flow behavior index (dimensionless)

$\left(\frac{\partial v}{\partial y}\right)$ = shear rate or velocity gradient

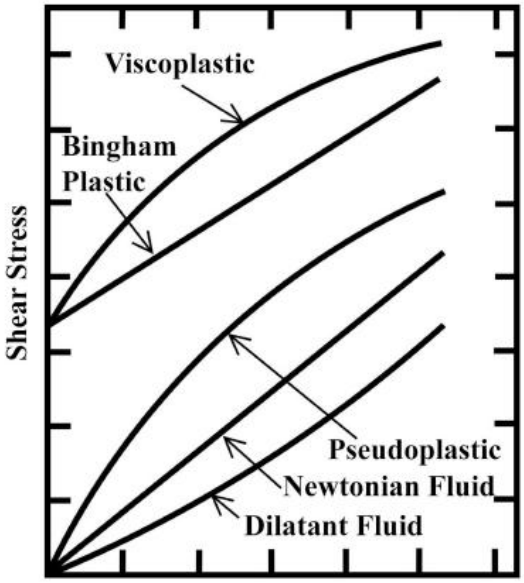

Figure 1.1 *Qualitative flow curves for different types of non-Newtonian fluids [27]*

1.1.2.1 Time-Independent behaviors:

(a).Bingham-plastic: These fluids oppose small forces to change their originality but flow easily under bigger shear stresses. Stress at which fluid is just in the condition of flow is known as yield stress. For example: tooth-paste, jellies.

(b). Pseudo-plastic: Mostly non-Newtonian fluids are pseudo-plastic in nature. For these fluids, viscosity reduces with amplification in velocity gradient. The well known example of pseudo-plastic fluid is blood. These fluids are also known as Shear thinning fluids because their viscosity is reduces rapidly with shear rate. For pseudo-plastic fluid, n is always less than 1 where n is flow behavior index.

(c). Dilatant fluids: For dilatant fluids, viscosity enhances with enhancement in shear rate. They are rare, but there are some examples like suspensions of starch and sand. These fluids are also known as shear thickening fluids. For dilatant fluids, n is always greater than 1.

1.1.2.2 Time reliant behaviors: These fluids are reliant upon extent of shear.

(a). Visco-elastic fluids: These are those types of fluids that have elastic properties, which allow them to come into their original position when a shear force is released. For example: white portion of egg.

(b). Rheopectic fluids: Fluids for which viscosity enhances with the increase in applied shearing force time are known as rheopectic fluids. Examples of the rheopectic fluids are suspension of gypsum in water.

(c). Thixotropic fluids: For these fluids, viscosity reduces as time (for application of shearing force) passes. Jelly paint solutions are the examples of these types of fluids.

1.2 Non-Newtonian flow over a bluff body

Heat and flow of fluid are usually moreover unbounded or bounded. A few problems associated with numerous of the properties of both unbounded and bounded flows. The unbounded flow pattern is an ordinary one for lowering and rising of temperature of fluids in numerous commercial uses. Buoyant force lays a great impact on flow and heat transfer properties when velocity of fluid is not very large and thermal gradient is relatively large. The influence of natural and forced convection is analogous in similar situations. The decay of vortices is also a matter of concern.

When the buoyant effects are added to the flow, it powerfully affects the flow and thermal structures. These effects are of prime importance in two situations when velocity is low and temperature gradient (from obstacle to flowing fluid) is very high. Buoyant effects are quantified by the parameter known as Richardson number. It yields demarcating line of natural convection from mixed one. The current study is concerned with the vertical flow of fluids ($n \leq 1$) around a cylinder of square cross section. The heat transfer is contributed by both kinds of convective modes (forced and natural). The geometry arrangement of single square cylinder can be categorized in common into the cylinders which are horizontaly placed and the cylinders which are tilted with an angle α from the horizontal.

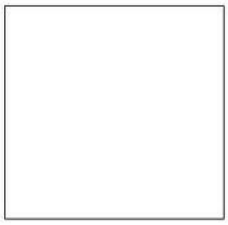

Figure 1.2: *Horizontal square cylinder*

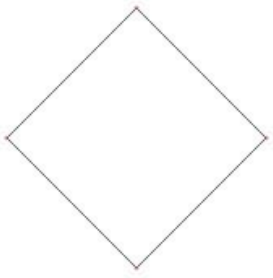

Figure 1.3: *Tilted square cylinder*

The most general arrangement of single square cylinders is the horizontal square cylinder, which is likely the arrangement most encountered in practice. The tilted square cylinder is not so common as the horizontal one.

1.3 Application

The case we are interested here is that of horizontal square cylinder which are very simple in configuration. Experimental analysis of the fluid flow and eddy dynamics about this simple configuration of single horizontal cylinder gives us the basic understanding about the flow around the buff bodies and it can be further implemented for more complex and larger scale structure such as two or more than two cylinders in side by side configuration. For illustration the flow across the tube banks working in process industries and particularly in power production and oil industry and river flow vegetation etc. Hence, the study of Reynolds number and Prandtl number (in case of heat transfer) would result in a clear understanding of many real life applications.

CHAPTER - 2

LITERATURE REVIEW

A vast amount of literature is available for the momentum and thermal exchange around obstacles of different cross sections impacted by buoyant force. **Badr [1]** studied heat transfer phenomena between flowing fluid and cylinder of circular cross section for the flow defined in laminar range. Two contradicting issues have been analyzed, first one is when the imposed flow is in the positive y-direction and second is when it directed vertically downwards. He reported that the upward flow regime is observed for the Reynolds number, Re = 5, 20, 40, 60 for the different values of Grashof number while there exist a downward flow. He analyzed the simulations for steady mixed convection flow for the parameters, Re = 1 – 40, Ri = 0 – 5 and Pr = 0.7 and reported that average Nusselt number shoots up to 41%. **Gandikota et al. [2]** has examined the upward flow of fluids ($n \leq 1$) with an immersed circular body. Buoyant force is incorporated in heat transfer properties from the circular body at different temperature from the fluid. They have studied the effect of aiding buoyancy which is characterized by $Ri > 0$ and opposing buoyancy which is characterized by $Ri < 0$. They take the range of engineering parameters as Ri = 0.5 to -0.5, Re = 50 to 150 with two values of blockage ratio (β) = 0.02, 0.25. It was found that flow around the cylinder shows an unsteady intermittent character in the preferred variation span of Re for free convection (Ri = 0). They also reported for the heat transfer, that there is an increase in Nusselt number at a more rapid rate outside the critical Ri, at the same time as it remains approximately constant in the opposing buoyancy case i.e. for $Ri < 0$. **Srinivas et al. [3]** examined the steady momentum transfer and thermal exchange properties between fluid and horizontal cylinder at a constant temperature for mixed convective case, which is engrossed in constant density non-Newtonian fluids. They performed the experiment in such a way that the direction of obligatory flow and the motion produced by the buoyancy effect are same. They have selected the ranges of parameters as the Re = 1 to 40, Ri = 0 to 2, n = 0.2 to 1.8, and Pr = 1 to 100. They stated that there is a similarity in the wake size behavior in the same manner as which was observed for special case of Ri = 0 which characterizes forced convection. They reported that both drag coefficients and average Nusselt number are reliant on the rising character of buoyancy property and the dimensionless flow defining factors like Prandtl

number. With the fluids with n = 0.2 to 2, they concluded that there is an increase in the drag coefficient and heat transfer with an increasing tendency of pseudo-plasticity of the fluid.

The present study incorporates a long square cylinder immersed in a flowing fluid. The literary body of knowledge is not scant for this shape of the bluff body although circular cylinder finds a wide industrial occurrence. **Okajima [4]** carry out an experiment to describe the unbounded flow across a cylinder of square cross section. He has taken the value of parameters as Re = $70-2\times10^4$. Further, he has utilized finite difference method to implement numerical simulations coupled with an isolated vortex scheme to determine the continuation of a transitional value of Re at which the flow patterns change drastically along with Strouhal number. **Nakabe et al. [5]** examined the buoyancy aided effect on the fluid flow limited by planar walls around a cylinder of circular cross section by the use of finite-difference scheme. The velocity at the inlet is defined by a parabolic equation so as to ensure the wall effects. They considered three flow patterns: **(a)** Influence of positive buoyancy at values of Reynolds number = 80 and 120, and Richardson number Ri = 0 to 1.6, and blockage parameter, β= 0.15 and 0.3; **(b)** Effect of negative buoyancy at Reynolds number = 50, Richardson number −1 to 0, and β= 0.15; and **(c)** Results of transverse-stream buoyancy for a fixed value of Reynolds number 80 and β= 0.3. They provided three important findings: First, that value of Richardson number which marks the decrease of eddy shedding collapse with enhancing value of β at fixed Reynolds number, second is the value of Richardson number at which eddy shedding collapse, augments with Reynolds number at constant β; and third one is the value of Reynolds number at which eddy shedding begins to raise with enhancing β at constant Ri. **Tamura et al. [6]** numerically predicted the non-uniform pressure distribution on the obstacle of square cross section with different inclinations. They have employed the direct finite difference scheme for the simulations in place of turbulence model. At very high Re = 10^4 - 10^6, to prevail over numerical unsteadiness, they introduced third-order upwind method for the convection terms. They reported that the computational outcome which explains phase variation on the surface of the cylinder mitigates to a great extent. This brings in complex correlations along the time-axis. But they could not find clear distinction in the variations in the variety of elevated frequency. **Abu-Hijleh [7]** numerically calculated the results for the laminar mixed convection correlations flow at unlike angles of hit for an constant temperature cylinder in traverse flow. This study covered a wide range of parameters: $1 \le \mathrm{Re} \le 200$, $0 \le © \le 35$ and $-® \le ¥ \le ®$, where κ is buoyancy parameter and γ is

angle of hit of fluid stream flowing towards the inward direction. They reported an alteration in the average Nusselt number, comparative to the situation of cross flow, increases about 20% for aiding buoyancy while it decreases up to 30% for opposing flows.

Turki et al. [8] analyzed the 2-D momentum transfer and thermal exchange between air which is laminar in nature flowing across a heated square cylinder. They have selected range of parameters for the study as Re = 62 – 200, Ri = 0 to 0.1 whereas the wall confinement was fixed at 0.25 and 0.125. The results demonstrated the occurrence of disintegration of the Karman vortex street as it also occurs for the square cylinder at a transitional value of Ri = 0.15, which was already reported in case of cylinder of circular cross section at Pr = 0.71. They established that the transitional value of Re comparative to the Re at which transition from steady to intervallic flow rises, when β increases, in pure forced convection. They found for the case of mixed convective thermal exchange, that the transitional Re compared to the value of Re which marks the changeover from steady to intervallic flow, reduces when there was an enhancement in Richardson number, While there was an amplification in the nature of Strouhal number (St) with rising Ri.

Sharma and Eswaran [9] studied the result of buoyant force effects on the flow configuration and thermal exchange nature across cylinder of square cross section in upward traverse flow. They studied the momentum transfer and thermal exchange uniqueness across a cylinder of square cross section kept at a fixed thermal condition. They investigated the influence of positive and negative buoyancy, for the range of parameters of Re = 100, Pr = 0.7 (fixed) and Ri = -1 to 1. They concluded that there is a wide difference in heat transfer nature in steady flow in comparison to the intervallic flow region, and later one has greater heat transfer. With increasing in Richardson number (Ri), they observed that the length of average circulation enhances in the intervallic flow, while it reduces uniformly in the steady flow range. They reported that the drag coefficient averaged over time axis becomes less than zero when value of Ri $\leq$ -0.25. They stated that there is an increasing nature of Strouhal number due to the fact that the speeding up on the surface of cylinder on boundary layer with increasing Ri. **Sharma and Eswaran [10]** have investigated the consequences of channel-confinement for varying wall confinement of 0.10, 0.30 and 0.50 on flow patterns around the square cross sectional bluff body. They have also studied heat transfer behaviors from a square cylinder at a relatively higher temperature by incorporating the buoyant force effects i.e. aiding for Ri greater than one and opposing buoyancy for Ri less than one. They have selected the parameters as Re = 100 and Pr = 0.7. To find out heat transfer characteristics,

they have examined the fact that surface Nusselt number enhances with increse in the channel confinement as well as Richardson number. **Paliwal et al. [11]** have researched steady, two dimensional and unbounded flows of non-Newtonian fluids fof n = 0.5 -1.4 around a square cross sectional cylinder. The range of engineering parameters employed are Re = 5, 10, 20, 30 and 40, Peclet numbers, Pe = 5 – 400 at fixed wall temperature as well as fixed heat flux. They have used finite difference scheme to discretize the governing differential equations. Afterward, **Dhiman et al. [12]** re-examined the same crisis by incorporating a much finer grid in a finite volume scheme. The parameters are varied as Reynolds number $1 \leq Re \leq 45$, power-law index $0.5 \leq n \leq 2$. The convective terms are discretized by using a higher order discretization scheme. Hence, findings by them are prone to be highly trustworthy as compared to **Paliwal et al. [11]**. In steady flow regime it can be deduced that, the effect of power-law index gradually mitigates as the Reynolds number increases. **Dhiman et al. [13]** explored the momentum transfer and thermal exchange behaviors of an isolated cylinder of square cross section placed symmetrically in a planar slit in cross flow. They selected the wide domain of limits as $1 \leq Re \leq 45$, $0.7 \leq Pr \leq 4000$ for Peclet number, $Pe \leq 4000$ and blockage ratio, $\beta = 0.125$, 0.167 and 0.25. They achieved relationships for thermal exchange in the non-variable flow region at isothermal conditions and fixed heat fluctuation state line situation on the square cylinder in cross flow. **Singh et al. [14]** calculated the buoyancy outcome on the wakes of circular and square cylinders for the range of Reynolds number, Re = 87 - 118 and Richardson Number, Ri = 0.049 - 0.173. They used temporally resolved schlieren imaging scheme to determine the qualitative flow visualization and quantitative measurements of dynamical behavior of vertical structures. It can be inferred that eddy formation behind the square/circular cylinder can be controlled by heating the cylinder. **Dhiman et al. [15]** considered the consequence of Pr on the momentum transfer and thermal exchange behaviors of a square cross sectional cylinder which kept at constant temperature confined within a channel under the influence of cross-buoyancy. They reported the mathematical results for the domain of engineering boundary as $1 \leq Re \leq 30$, $0.7 \leq Pr \leq 100$ for the maximum value of Peclet number = 3000 and Richardson number, $0 \leq Ri \leq 1$ for a wall confinement of 12.5%. They stated that effect of the Ri on the drag coefficient and the Nusselt number is as analogous as in the matter of the unbounded mixed convective case. For the domain of parameters deliberate by them, they reported that the rate of Nusselt number increased about 5% with reference to the convection defined by Ri = 0. **Biswas et al. [16]** examined the eddy formation around a cylinder with temperature gradient in a transverse-

flow at low Re in the presence of thermal buoyant force. They have taken the option of Re as 10 to 45. They found that the flow shows a non changing behavior in the nonexistence of thermal buoyant force. They reported that asymmetry of wake and periodicity of flow can happen at minor Re in comparison to convection defined by Ri = 0. **Paramane and Sharma [17]** investigated the consequences of revolution on the momentum transfer and thermal exchange across a cylinder in the presence of transverse-stream buoyant force. They have examined the buoyancy-induced eddy formation across the revolving cylinder in the fixed wall temperature state. They have taken air as the working fluid while the the range of engineering parameters for which the study is carried out as Re = 40 to 100 and dimensional-less rotational velocity (α) was changing from 0 to 8 and Ri was taken as, Ri = 0 - 1. They reported that the Nusselt number shows an inverse relation with rotation at the same time as it shows a proportional relation i.e. it increases with buoyancy effect. **Sarkar et al. [18]** numerically examined the mixed convective heat transfer from two identical square cylinders in cross flow. The range of parameters was taken as Re = 100, Pr = 0.7 and Richardson number, Ri = -1 to 1 has been taken. They stated that for meticulous cylinder spacing, vortex shedding is observed up to Richardson number of 0.25. From their report, the highest heat transfer set up at the front face of second cylinder. **Rao et al. [19]** considered momentum transfer and thermal exchange from a square cross sectional cylinder for the non-Newtonian fluids. They presented the results on streamline and vorticity contours around the obstacle. They have chosen an array of engineering parameters as Reynolds number, Re = 0.1 – 40, Pr = 0.7 – 100 and n = 0.2 – 1.4. They concluded that there is a need of a longer upstream region as the value of the Reynolds number is gradually reduced for obtaining the results which are free from numerical errors. **Dhiman et al. [20]** calculated the wall property across the square cross sectional cylinder at steady flow situation in the presence of transverse buoyant force. They performed numerical simulations in the non-changing flow field for the array of Re = 1 – 30, Ri = 0 to 1 for blockage ratios of 0.125 and 0.25 at a constant Pr = 0.7. They reported that cylinder average Nusselt number is insensitive towards the variation of the values of the Richardson number for the constant values of Reynolds number and the blockage ratio.

Chatterjee and Mondal [21] examined the influence of thermal buoyant force on the momentum transfer and thermal exchange. They observed the eddy formation at the rear of a cylinder of square cross section in traverse flow. They take a low range of Reynolds numbers for the study. They have taken the range of engineering parameters, Reynolds and Richardson numbers as Re = 5 to 40 and Ri = 0 to 2 while taking the unchanging value of Pr = 0.7 and a

β = 0.05. They concluded that the Nusselt number found to be escalating in nature with Reynolds number. The reason behind that the elevated heat transfers due to the augmented convection by the fluid. It can be easily examined that average Nusselt number is found to increase a little under the vital Ri, while the quickness of amplification in Nusselt number increases above the vital Ri. **Sasmal and Chhabra [22]** investigated the orientation effect on laminar natural convection from a heated square cylinder in power-law fluids. They performed numerical simulation on the governing differential equations describing the fluid flow and heat transfer over broad domain of non-dimensional variables like Grashof number, Gr = 10 to 10^5, Prandtl number, Pr = 0.72 to 100 and n = 0.3 to 1.8. They concluded that a square cylinder at α = 0 experiences more drag than that at α = 45° under the same conditions. **Sharma et al. [23]** premeditated the consequence of positive buoyant force on the mixed convection momentum transfer and thermal exchange across a long cylinder of square cross section in the vertical unconfined model. They reported the results for the wide domain of variables as Re = 1 to 40 and Ri = 0 to 1 at the constant Pr = 0.7. They stated that the wake length reduces on enhancing the Ri for a fixed value of Re. They also stated that the local Nu is lower for the forced convective case in comparison to the convective case defined by Ri = 0.5 and 1. The drag coefficient is found to be diminish with elevated values of Re but this drag coefficient shows an inverse trends i.e. it enhances with enhancement in value of Richardson number.

Thus, from the above discussion, it can be summarized only **Sharma and Eswaran [9], Singh et al. [14]** and **Sharma et al. [23]** have researched with supportive buoyant force around a cylinder of square cross section in the unsteady unconfined perpendicular flow system. Still, conversely, there is no work existing entire research work for the square bluff body in the presence of buoyant force given by Ri > 0 in the non-Newtonian unsteady unbounded domain. Therefore, the purpose of the current research is to explore the effect of positive buoyant force on momentum transfer and thermal exchange for the fluid defined by power-law index, n < 1 around a square cylinder at Reynolds numbers, Re = 75 to 150 and Richardson number, Ri = 0 to 1 for the fixed Prandtl number, Pr equel to 50.

CHAPTER - 3

METHODOLOGY

3.1 Problem statement and governing equations

Suppose the two dimensional physical model of unsteady, forced flow over a heated long square cross sectional cylinder (size D) at a fixed temperature T_w in a non-Newtonian fluid flowing upwards in opposition to gravity. The streaming fluid has uniform temperature T_∞ and velocity U_∞ as shown in figure 3.1. For physical understanding of the model, it is required to execute unbounded flow condition, the bluff body is artificially restricted by two symmetric slip walls. The square bar is kept at a constant temperature of T_w .The total height of the channel in upstream and downstream direction are symbolized by L (= X_u+X_d). The space from the entering space to the front face of the bluff body is X_u and the space between the rear surface of the bluff body and the outlet space is X_d. The dimensions of the channel are so selected that mitigate the consequence of the inlet and exit edge circumstances on the flowing pattern near the cylinder. Cylinder is centered at downstream distance X_d on the vertical symmetric axis.

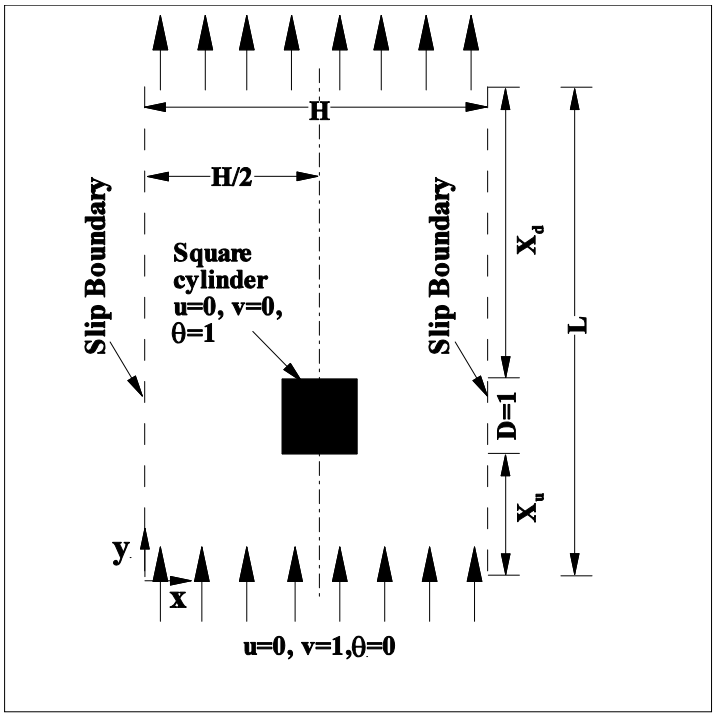

Figure 3.1: *Schematic diagram for the present system*

The bluff body experiences buoyant force owing to the density difference (with temperature) near the square cylinder. Heat transfer is purely by natural convection at Re = 0 (no imposed flow) while at high Re buoyant forces are insignificant (forced convection). It is obvious that there exists in between both free and forced convection; the proportion of which is determined by another parameter Richardson number (Ri). As we are considering the buoyant force effect owing to the density difference we cannot assume constant density (ρ). A well known Boussinesq expression, $\rho = \rho_0(1 - \beta(T - T_0))$ gives the density variation with temperature but this can be applied only when the change in the density is not very large. Here ρ_0 is the density at the reference temperature (T_0). At constant transport properties viscous rakishness are minor and the thermo-physical properties except density (heat capacity c, thermal conductivity k, viscosity, non-Newtonian flow parameters m, n) are taken as to be independent of thermal gradient. With both two assumptions, we are restricted to apply the above model only for small temperature differences and low to moderate viscosity levels.

In the presence of these circumstances, the momentum and heat transfer incident are directed by the continuity, momentum and thermal energy equations, presented here in their dimensional type as follows:

(a). Continuity Equation:

$$\nabla . U = 0 \qquad \textbf{(1)}$$

(b). Momentum Equation:

$$\circ\left(\frac{\partial U}{\partial t} + U.\nabla U - \P\right) - \nabla .\pm = 0 \qquad \textbf{(2)}$$

(c). Energy Equation:

$$\rho C_p\left(\frac{\partial T}{\partial t} + U.\nabla T\right) - k\nabla^2 T = 0 \qquad \textbf{(3)}$$

where ° is the density of the fluid, U is the velocity of flowing fluid with its components U_x and U_y in x- and y axis, respectively, ¶ is the body force, ± is the stress tensor and T is the temperature. The stress tensor ± is defined as the sum of the isotropic pressure p and the deviatory stress tensor ² and is given by Eq. (4)

$$\pm = -pI + ²$$ **(4)**

For incompressible fluids, the rheological equation of state is given as

$$² = 2¦£(U)$$ **(5)**

where $¶(U)$, is the components of the rate of strain tensor and defined by Eq. (6)

$$£(U) = \frac{1}{2}\left[(\nabla U) + (\nabla U)^T\right]$$ **(6)**

The viscosity ¦, for power-law fluids, is given by Eq. (7)

$$¦ = m\left[\frac{I_2}{2}\right]^{(n-1)/2}$$ **(7)**

Where n is the non-Newtonian flow index of the fluid (n < 1 means to a pseudo-plastic fluid; n = 1 involve Newtonian fluid; n > 1 direct to a dilatant fluid), m is the non-Newtonian fluid consistency index and I_2 is the second invariant of straining rate tensor£, which is defined by $I_2 = 2(£_{xx}^2 + £_{yy}^2 + £_{xy}^2 + £_{yx}^2)$. The mechanism of the straining rate tensor is associated to the velocity factorss in Cartesian coordinates as pursues:

$$£_{xx} = \frac{\partial U_x}{\partial x}; £_{yy} = \frac{\partial U_y}{\partial y} \& £_{xy} = £_{yx} = \frac{1}{2}\left(\frac{\partial U_x}{\partial y} + \frac{\partial U_y}{\partial x}\right)$$

Boundary Conditions:

The dimensional boundary circumstances for unbounded constant temperature momentum transfer and thermal exchange across a square cross sectional cylinder may be given in following form:

At the inlet boundary: $U_x = 0$, $U_y = U_\infty$ and $T = T_\infty$ (isothermal flow) **(8)**

On left and right margins: $U_x = 0$, $\partial U_x/\partial x = 0$ and $\partial T/\partial x = 0$ **(9)**

On the exterior of the square cylinder: $U_x = 0$, $U_y = 0$ and $T = T_w$ **(10)**

At the exit boundary: $\partial U_x/\partial y = 0$, $\partial U_y/\partial y = 0$ and $\partial T/\partial y = 0$ **(11)**

3.2. Numerical methodology

The principal equations have been solved numerically using finite volume scheme oriented commercial package ANSYS FLUENT. In the present study, the computational grids with diamond cells of non-homogeneous spacing are created by the use of industrial grid unit GAMBIT. The fine grid size of 0.005D is clustered around the square bluff body to highlight the boundary layer effects. The two-directional, unsteady, laminar scheme is used to solve the

constant density flow on the grid configuration. Quadratic upwind differencing method (QUICK) is used to simulate the convective components of the correlation of the momentum and energy. A semi-implicit scheme for the pressure coupled relationships (SIMPLE) was taken for explaining the pressure-velocity decoupling.

Power-law model is implemented to incorporate the non-Newtonian behavior and density variation is effected by the Boussinesq expression. The maximum error standard of 10^{-20} is used for the continuity element; and same for *x*-and *y* directional factors of the velocity and temperature have been followed in the study. Also it has been assumed that the solution has converged if there is no variation up to 4^{th} digit in the drag values and at the same time lift coefficients are of the range 10^{-5} to 10^{-6} when it has shown more than 10 series in time record. The non uniform computational grid for the present study is shown in figure 3.2.

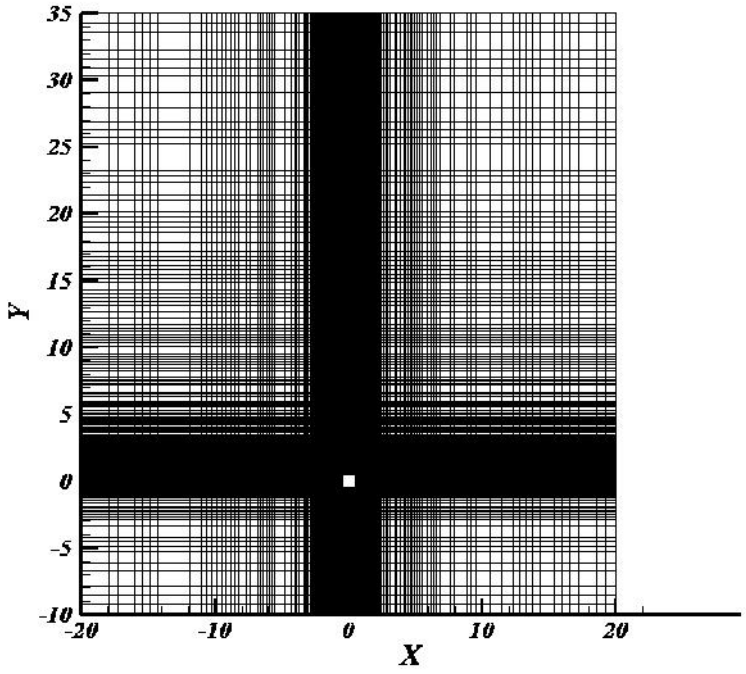

Figure 3.2: *Non-uniform computational grid arrangement across the square cylinder*

3.3. Grid dependence Study

The grid dependence study is performed with three non-uniform grids having total number of cells (104625,117500,130375 with 75,100,125 control volumes across the square cylinders) at Reynolds number Re=150 and Richardson numbers Ri = 0 and 1. Table 3.1 clearly shows that at Ri = 0 the drag coefficient (C_D) bears the percentage deviation of about 0.04% for control volume CV = 100 which is less than 0.18% at CV = 75. Similar behavior is shown at Ri = 1 with 0.13% deviation at CV=100. Further, at Ri = 0 the time-averaged Nu shows a percentage deviation of about 0.23% for control volume CV = 100 which is less than 0.35% at CV = 75. Similarly at Ri = 1, the deviation is 0.23% at CV = 100 in comparison to 0.31% for CV = 75. Hence, considering the computational span required and the exactness of the results obtained, the present statistical study is conducted for the grid range of total cells 117500 with CV = 100 on every side of the square cylinder.

Table 3.1: Grid dependence test for Ri=0 and 1 at Re=150 and Pr=50

S. No.	Grid size (cells)	CV on each side of square obstacle	C_D	% deviation	Nu	% deviation
Ri=0						
1	104625	75	1.4657	0.18	20.4292	0.35
2	117500	100	1.4637	0.04	20.4044	0.23
3	130375	125	1.4631		20.3572	
Ri=1						
1	104625	75	1.6012	0.25	24.9852	0.31
2	117500	100	1.5993	0.13	24.9661	0.23
3	130375	125	1.5972		24.9077	

3.4. Upstream and Downstream dependence studies

Effect of upstream and downstream space on the present numerical analysis is carried out to ensure that the results are free from any domain effects. Upstream dependence study is employed for the upstream distances of 5.5D (106500 cells), 10.5D (117500 cells) and 15.5D (129400 cells) at Re=150 and a fixed value of Pr = 50 for a range of Richardson number, Ri = 0, 1. At X_u = 10.5D, the relative divergence in the time-averaged cylinder Nu and total drag coefficient are reported to be less than 0.52% and 2.16% respectively at Ri = 0 in comparison with X_u = 15.5D at X_d = 35.5D and H = 40D, while deviation in same parameters is 1.11% and 3.65% respectively for the X_u = 5.5D. Similar observation at Ri = 1 states the relative percentage deviations in the average cylinder Nu and total C_D to be 1.26% and 0.3% for X_u =

10.5D and for X_u = 5.5D it is 2.01% and 0.41%. Hence, it is wise to use the upstream space of 10.5D for the production of novel outcome.

Downstream dependence study is conducted for the distances of 30.5D (110500 cells), 35.5D (117500 cells) and 40.5D (124300 cells) at Reynolds number Re = 150 and Prandtl number Pr = 50 at Richardson number Ri = 0, 1. At X_d = 35.5D, the comparative variation in the time-averaged cylinder Nu and total C_D reported are less than 0.003% and 0.01% respectively at Ri = 0 in comparison with X_d = 40.5D at X_u = 10.5D and H = 40D while deviation in same parameters is 0.02% and 0.05% respectively for the X_d = 30.5D. Similar observation at Ri=1 states the relative percentage deviations in the average cylinder Nusselt number and total drag coefficient to be 0.002% and 0.007% for X_d = 35.5D, while for X_d = 30.5D, it is 0.004% and 0.03% respectively. Therefore, the downstream distance is fixed to be 35.5D. These results are shown in Table 3.2.

Table 3.2: Domain dependence test for Ri=0 and 1 at Re=150 and Pr=50 for CV=100

S. No.	Grid Size (cells)	Length	C_D	% deviation	Nu	% deviation
Ri=0						
X_u Effect						
1	106500	5.5D	1.4852	3.65	20.5247	1.11
2	117500	10.5D	1.4637	2.15	20.4044	0.52
3	129400	15.5D	1.4329		20.2994	
X_d Effect						
1	110500	30.5D	1.4632	0.05	20.3998	0.02
2	117500	35.5D	1.4637	0.01	20.4044	0.003
3	124300	40.5D	1.4639		20.4037	
H Effect						
1	52500	20D	1.4853	3.45	20.4794	0.82
2	117500	40D	1.4637	1.95	20.4044	0.45
3	182700	60D	1.4358		20.3128	
Ri=1						
X_u Effect						
1	106500	5.5D	1.6113	2.01	24.9953	0.41
2	117500	10.5D	1.5994	1.26	24.9661	0.30
3	129400	15.5D	1.5795		24.8924	
X_d Effect						
1	110500	30.5D	1.5997	0.03	24.9668	0.004
2	117500	35.5D	1.5994	0.007	24.9661	0.002
3	124300	40.5D	1.5993		24.9657	
H Effect						
1	52500	20D	1.6073	1.45	24.9827	0.18
2	117500	40D	1.5994	0.95	24.9661	0.12
3	182700	60D	1.5843		24.9373	

3.5. Computational Domain Width

After fixing the upstream and downstream distances the width of domain is further checked to yield reliable results. Domain width is varied as, H = 20D (52500 cells), 40D (117500 cells) and 60D (182700 cells) in the x - direction (upward flow). The parameters used in this analysis are Re = 150 and fixed Pr = 50 at Ri = 0 and 1. At H = 40D, the relative percentage divergence in the time-averaged cylinder Nu and total C_D reported are less than 0.45% and 1.95% respectively at Ri = 0 in comparison with H = 60D at X_u = 10.5D and X_d = 35.5D while the deviation in same parameters is 0.82% and 3.45% respectively for the H = 20D. Similar observation at Ri = 1 states the relative percentage deviations in the average cylinder Nusselt number and total drag coefficient to be 0.12% and 0.95%,while for H = 20D, it is 0.18% and 1.45% respectively. Hence the computational domain defined by X_u = 10.5D, X_d = 35.5D and H = 40D is found to be efficient enough to carry out the present investigation.

CHAPTER - 4

RESULTS AND DISCUSSION

In present study, simulations are performed for Reynolds number, Re = 75 - 150 in the step of 25 and power-law index (n) = 0.2, 0.4, 0.6 and 1 to show the influence of non-Newtonian behavior characterized by n < 1 (Pseudo-plastic fluids) on the vertical flow around the square bluff body. The effect of Richardson number (Ri), power-law index (n) on streamlines and isotherm contours is studied thoroughly.

4.1. Validation of Results

Table 4.1, shows the comparison of drag coefficient and Nusselt number for mixed convection in the range Re = 100, Pr = 0.7 and Ri = 0 and 1 in the two dimensional vertical unconfined domain with literature value. A superb conformity is found among the current study and that of **Sharma and Eswaran [9]** and **Chatterjee and Mondal [21]**. The percentage deviations are found to be about 1.1% for drag coefficient, and about 0.52% and 0.81% for Nusselt number in both studies at Ri = 0. However, the percentage deviations is found to be about 0.35% for drag coefficient and about 3.87% and 0.37% for Nusselt number in both studies respectively at Ri = 1. The slight disparity between these studies is attributed to the unlike channel dimension and time step.

Table 4.1: Comparison of current outcomes with literature value for Re=100, Pr=0.7 and Ri=0 and 1

Source	**C_D**	**% deviations**	**Nu**	**% deviations**
Ri=0				
Present study	1.4925		4.0191	
Sharma and Eswaran [9]	1.5092	1.11	3.9984	0.52
Chatterjee and Mondal [21]	-	-	3.9868	0.81
Ri =1				
Present study	2.6438		4.8637	
Sharma and Eswaran [9]	2.6346	0.35	4.6823	3.87
Chatterjee and Mondal [21]	-	-	4.8457	0.37

Further, Table 4.2 presents the comparison of C_D and cylinder Nu for convective heat transfer defined by Ri = 0 at Re = 10 and 40 with **Sharma et al. [23]** and **Dhiman et al. [24]**. Again, a close correspondence is observed between three studies in Table 4.2. The highest divergence in the values of C_D and cylinder Nu observed are around 0.52% and 0.38% for Re = 10 and it has found 4.05% and 2.52% for Re = 40.

Table 4.2: Comparison of current outcomes with literature value for Pr=0.7, Ri=0 and Re=10 and 40

Source	Re	C_D	% deviations	Nu	% deviations
Present study	10	3.2728		1.5565	
Sharma et al.[23]	10	3.2898	0.52	1.5573	0.05
Dhiman et al.[24]	10	3.2599	0.39	1.5624	0.38
Present study	40	1.7088		2.6666	
Sharma et al.[23]	40	1.7809	4.05	2.6012	2.52
Dhiman et al.[24]	40	1.7668	3.28	2.6969	1.12

Further, Table 4.3 presents the comparison of drag coefficient, Strouhal number and Nusselt number for convective case defined by Ri = 0 at Re = 100 and power-law index, n = 0.5, 0.6 and 0.8 with **Sahu et al. [25].** Again, a close correspondence is observed between two studies in Table 4.3. The upper limit of the digression in the C_D, Strouhal number and time-averaged cylinder Nu is about 4.48%, 3.77% and 0.64% for Re=100.

Table 4.3: Comparison of current outcomes with literature value for Pr=50, Ri=0 and Re=100

Source	C_D	% error	St	%error	Nu	% error
n=0.5						
Present study	1.5515		0.1289		22.3668	
Sahu et al.[25]	1.6243	4.48	0.1339	3.77	22.2247	0.64
n=0.6						
Present study	1.3975		0.1475		-	
Sahu et al.[25]	1.4482	3.50	0.1496	1.40	-	
n=0.8						
Present study	1.4177		0.1515		18.0654	
Sahu et al.[25]	1.4433	1.77	0.1558	2.76	17.9642	0.56

4.2. Flow Patterns

Unsteady streamline profiles in the region surrounding the submerged square cylinder are shown in Figures 4.1 - 4.4 for shear thinning behavior of fluid. Values of different parameters are non-Newtonian flow index (n) = 0.2, 0.6, 0.4, 1, Reynolds number (Re) = 75, 100, 125, 150 and Richardson number (Ri) = 0, 0.5, 1. The instantaneous wake size is seen to be smallest for n = 0.2 (shear-thinning fluid) and the largest for n = 1 (Newtonian fluid) at Re = 75. It is easily inferred that the wake size is enhanced in both length and width with fluid manners converted from pseudo-plastic (n < 1) to Newtonian (n = 1) for a particular Reynolds number (Re). A qualitative explanation is provided for the above phenomena. Shear-thinning fluids experience lesser viscosity in the surrounding area of the exterior of the cylinder and this slowly rises away from the cylinder with the decreasing shear rate. Thus, it

can be deduced that, shearing is restricted to a small region in the vicinity of the cylinder which is surrounded by a highly viscous region. As expected, this virtual confinement suppresses wake region. This clearly explains the mitigation of wake region with increasing power-law index (n). Furthermore, the flow field shows periodicity in the entire Reynolds number range $(75 \leq \mathrm{Re} \leq 150)$ in the present study, which is well in line with literature [26].

Flow separation commences from fixed corners of the square cylinder and two asymmetric (about the mid-plane) wakes form at its rear end. This observation is well correlated with the existing study of Chandra and Chhabra [26] who have observed similar periodicity with semi-circular cylinder. Wakes form in due course of time, grow and alternatively break off from the main body. The trend is repeated after a fixed time interval thereby contributing to periodic nature. Owing to increased frequency of vortex shedding at high Reynolds numbers, two wakes are seen to be attached at the rear surface at Ri = 0. While at Re = 150, Ri = 1 the number of these wakes reduces to one. Hence, it is obvious that increasing turbulence and the degree of mixed convection, reduces the wake number.

Figures 4.1 – 4.4 represents the streamline patterns for range of Re = 75 – 150, n = 0.2 – 1.0, Ri = 0 – 1 and Pr = 50 (fixed value). It can be noted from Figure 4.1 (a – l) that for the range of Re = 75 – 150, the flow is unsteady for all Ri at n = 0.2. However, for n = 0.4 flow is steady for Ri = 0.5 and 1 (Figure 4.2 b, c) while it is unsteady for Ri = 0 (Figure 4.2 a). Also it can be noted from Figure 4j that the flow is symmetric about the central axis for Reynolds number of 100 and Richardson number of 1. For all other Re and Ri at n = 0.4, the flow is unsteady. It can also be noted the flow is steady for Re = 75 and Ri = 0.5, 1 at n = 0.6, 1 (Figure 4.3 – 4.4). This is well matched with Chandra and Chhabra [26] where similar profiles have been obtained.

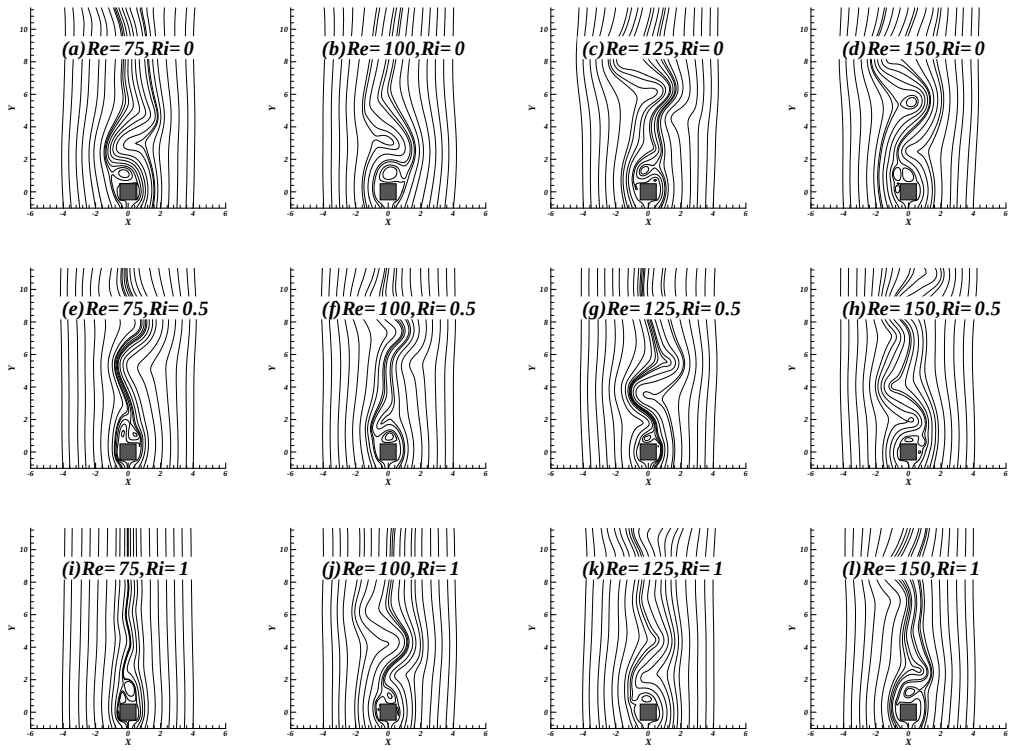

Figure 4.1: *Representative (a-l) streamlines contours for n=0.2 at constant Pr =50*

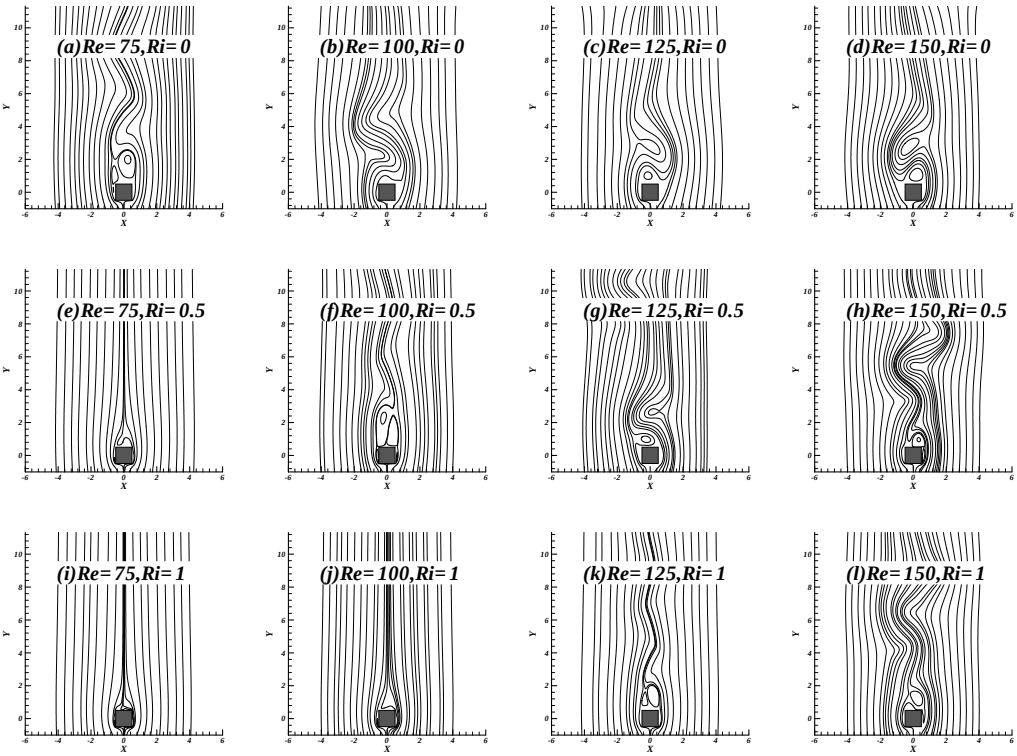

Figure 4.2: *Representative (a-l) streamlines contours for n =0.4 at constant Pr =50*

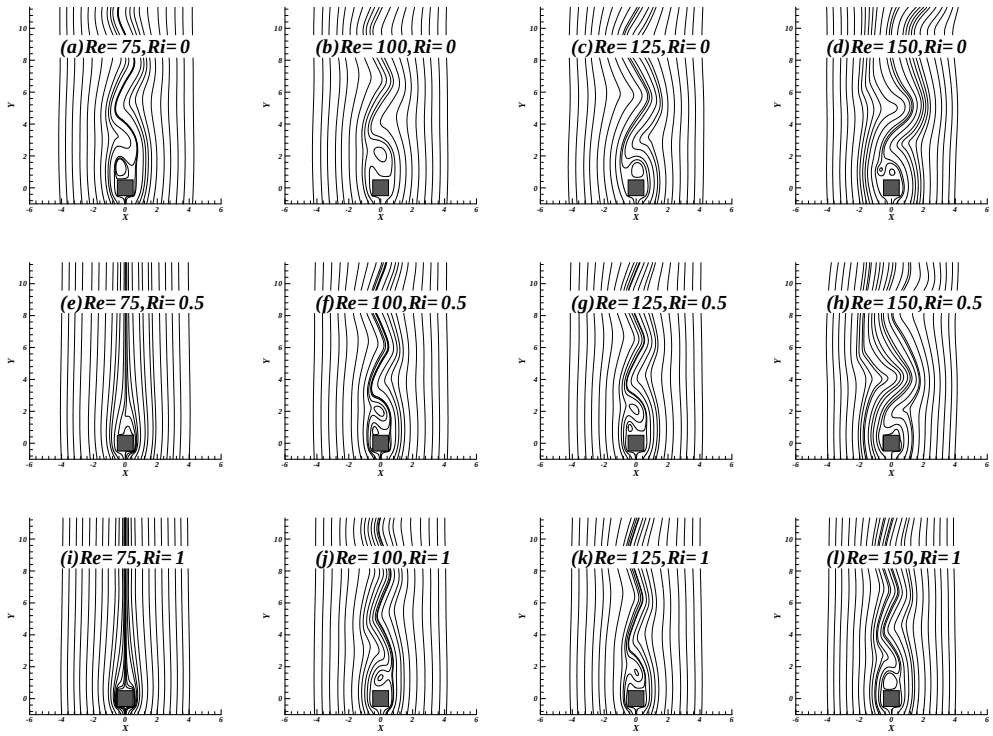

Figure 4.3: *Representative (a-l) streamlines contours for n=0.6 at constant Pr =50*

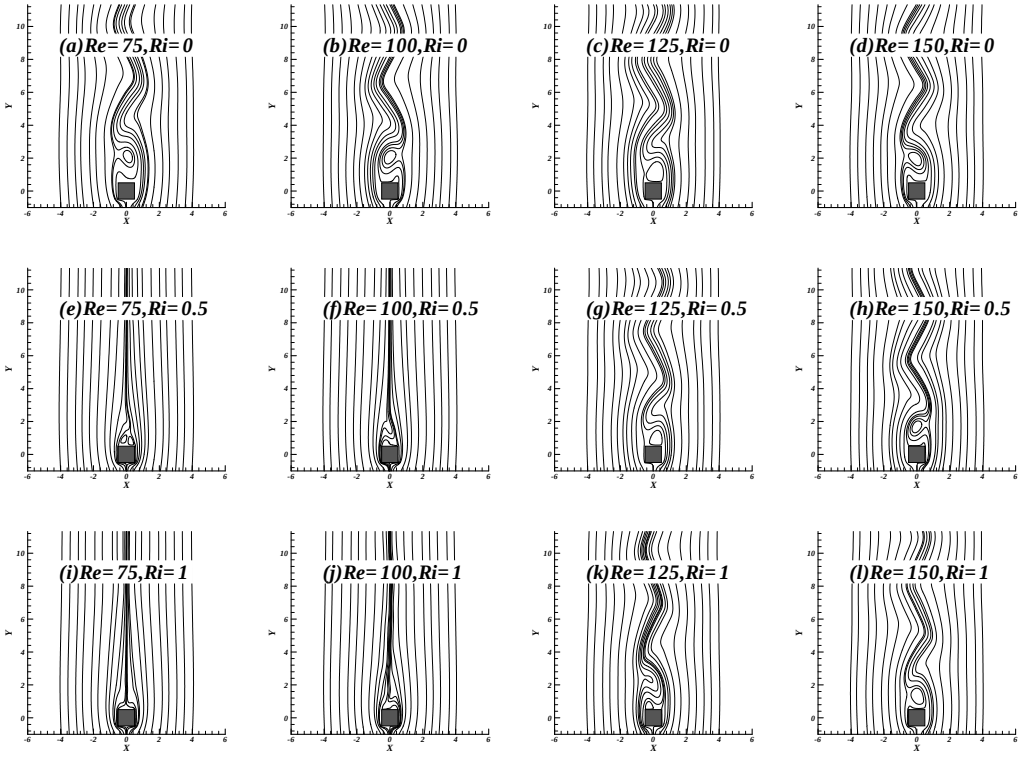

Figure 4.4: *Representative (a-l) streamlines contours for n=1 at constant Pr =50*

4.3. Thermal Patterns

Isotherm profiles are used to depict the temperature field near the bluff body. The isotherms crowd in the upstream way with growing value of Reynolds number, and/or Prandtl number. This shows that the heat transfer increases with escalating Re as well as Pr due to increase in turbulence, temperature gradient. The effect of non-Newtonian flow index on isotherm profiles is observed to be largely prominent at higher values of Re, Pr. The shear-thinning nature of fluid, described by the power-law index ($n < 1$) enhances heat transfer due to progressive thinning of thermal boundary layer near the bluff body as n decreases.

Figures 4.5 – 4.8 represents the isotherm patterns for range of Re = 75 – 150, n = 0.2 – 1.0, Ri = 0 – 1 and Pr = 50 (fixed value). It can be noted from Figure 4.5 (a – l) that for the range of Re = 75 – 150, the flow is unsteady for all values of Ri at n = 0.2. However, for n = 0.4 flow is steady for Ri = 0.5 and 1 (Figure 4.6 b, c) while it is unsteady for Ri = 0 at all values of n = 0.2, 0.4, 0.6, 1 (Figure 4.6 a). Clustering of isotherms at the front end of the cylinder directly implies elevated temperature gradients thereby high value of local Nusselt number. Downstream area shows periodicity of isotherm layers. The recirculating region is seen to increase as flow transits from shear thinning to Newtonian behavior. A direct offshoot of this recirculating region is the suppression of transverse oscillations. Also it can be noted from Figure 4.6 j that the flow is symmetric about the central axis for Reynolds number of 100 and Richardson number of 1. For all other Re and Ri at n = 0.4, the flow is unsteady. It can also be noted the flow is steady for Re = 75 and Ri = 0.5, 1 at n = 0.6, 1 (Figures 4.7 – 4.8). This is also well matched with Chandra and Chhabra [26] where similar profiles have been obtained.

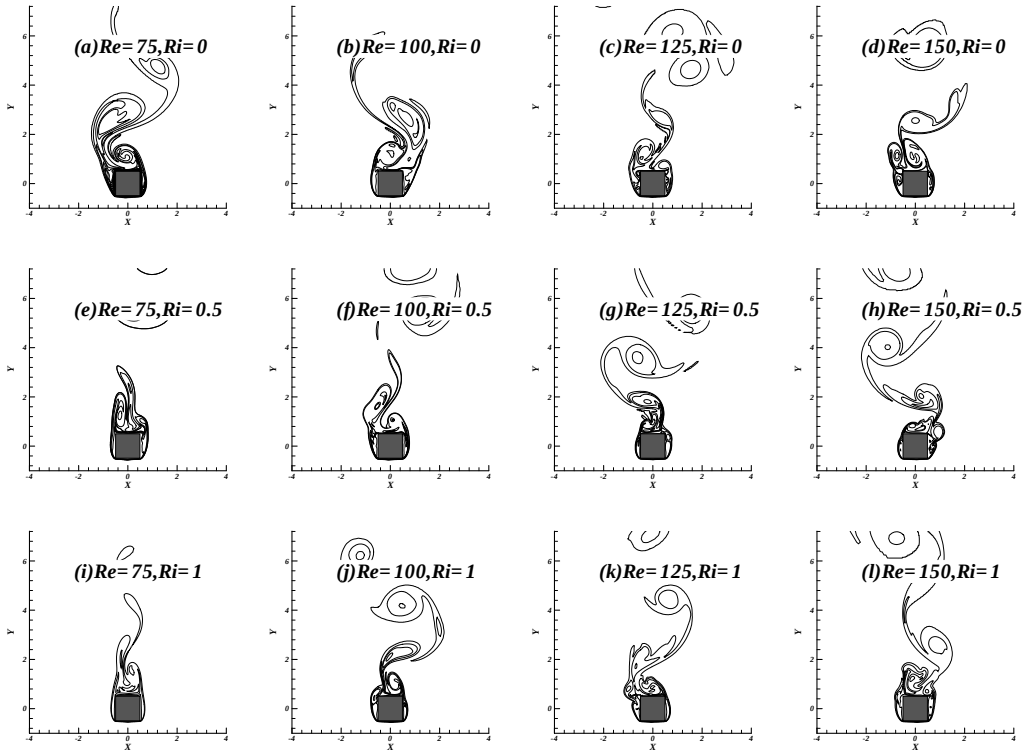

Figure 4.5: *Representative (a-l) isotherms profiles for n=0.2 at constant Pr =50*

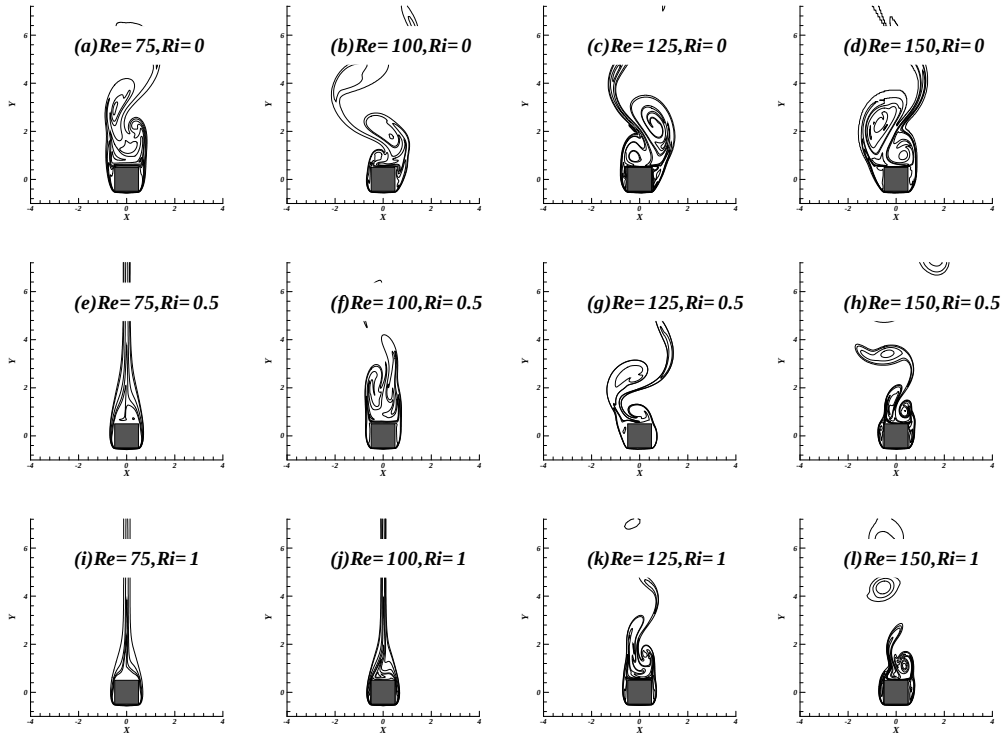

Figure 4.6: *Representative (a-l) isotherms profiles for n=0.4 at constant Pr =50*

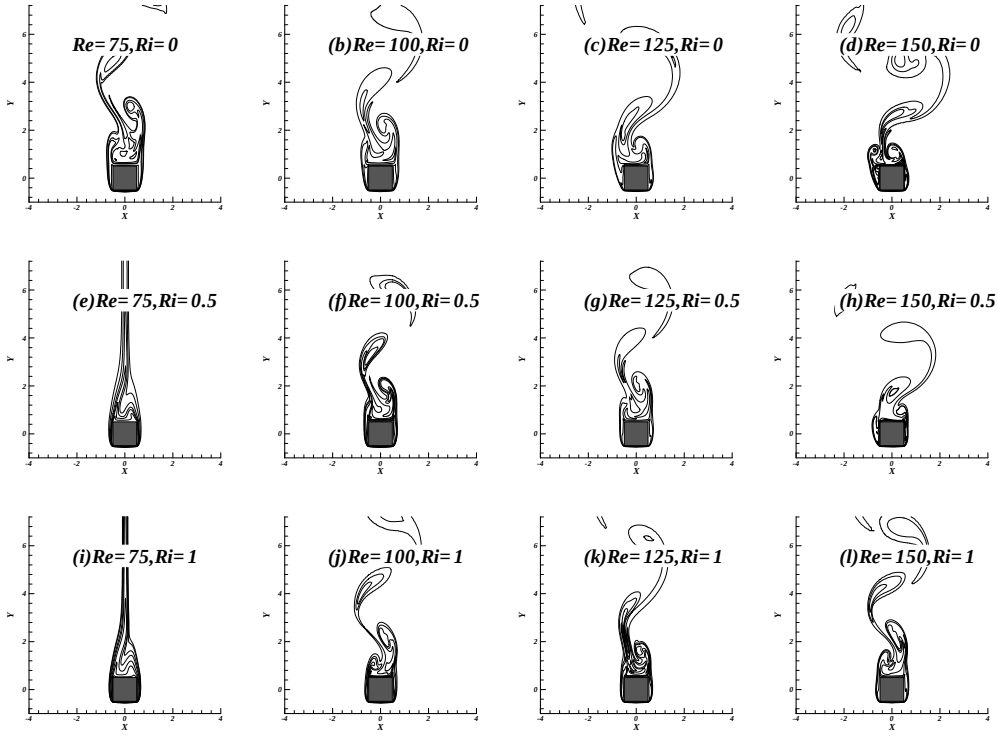

Figure 4.7: *Representative (a-l) isotherms profiles for n=0.6 at constant Pr =50*

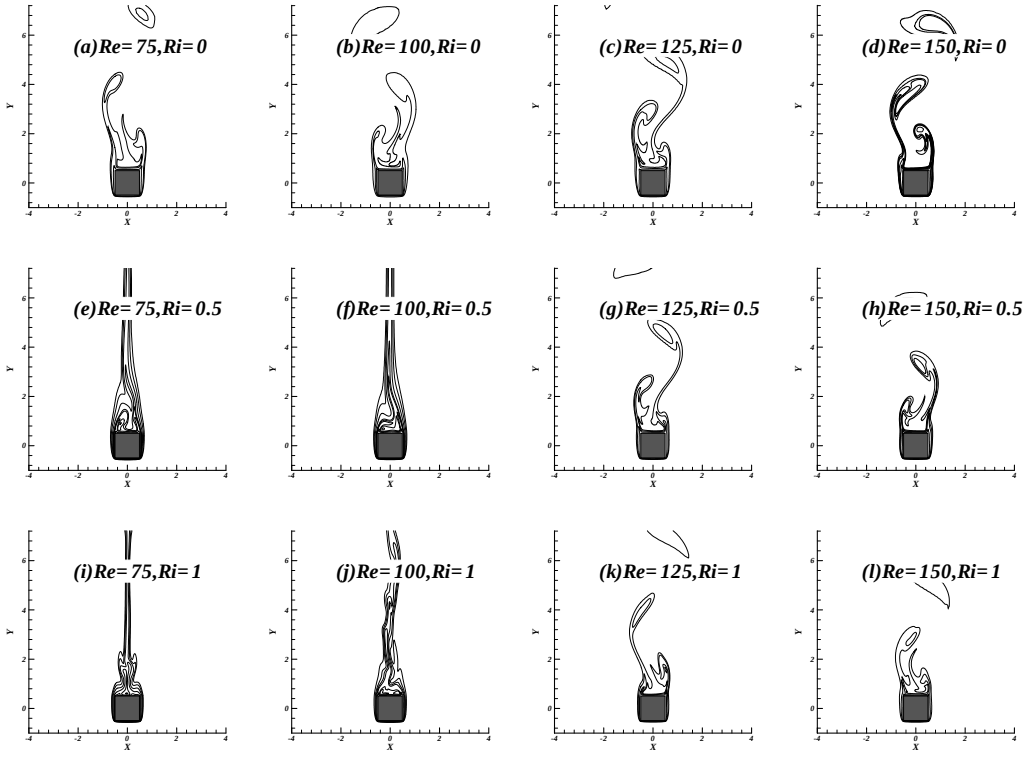

Figure 4.8: *Representative (a-l) isotherms profiles for n=1 at constant Pr =50*

4.4. Individual and Total Drag Coefficient (C_D)

For a constant Re, the total drag coefficient (C_D) is found to decrease with increasing nature of shear-thinning behavior of fluid. This behavior is observed for the range of Ri studied i.e. Ri = 0 to 1. We can also see the similar trend (decreasing C_D) for the nature of flow moving from mixed convection (Ri = 1) to pure forced convection (Ri = 0). Friction drag coefficient is clearly seen to decrease with increasing Re. For a particular value of Ri it enhances with rising power-law index. As already seen that n is found to have a strong influence at low Re as at a higher value because the effect of viscosity is reduced at higher values of Re.

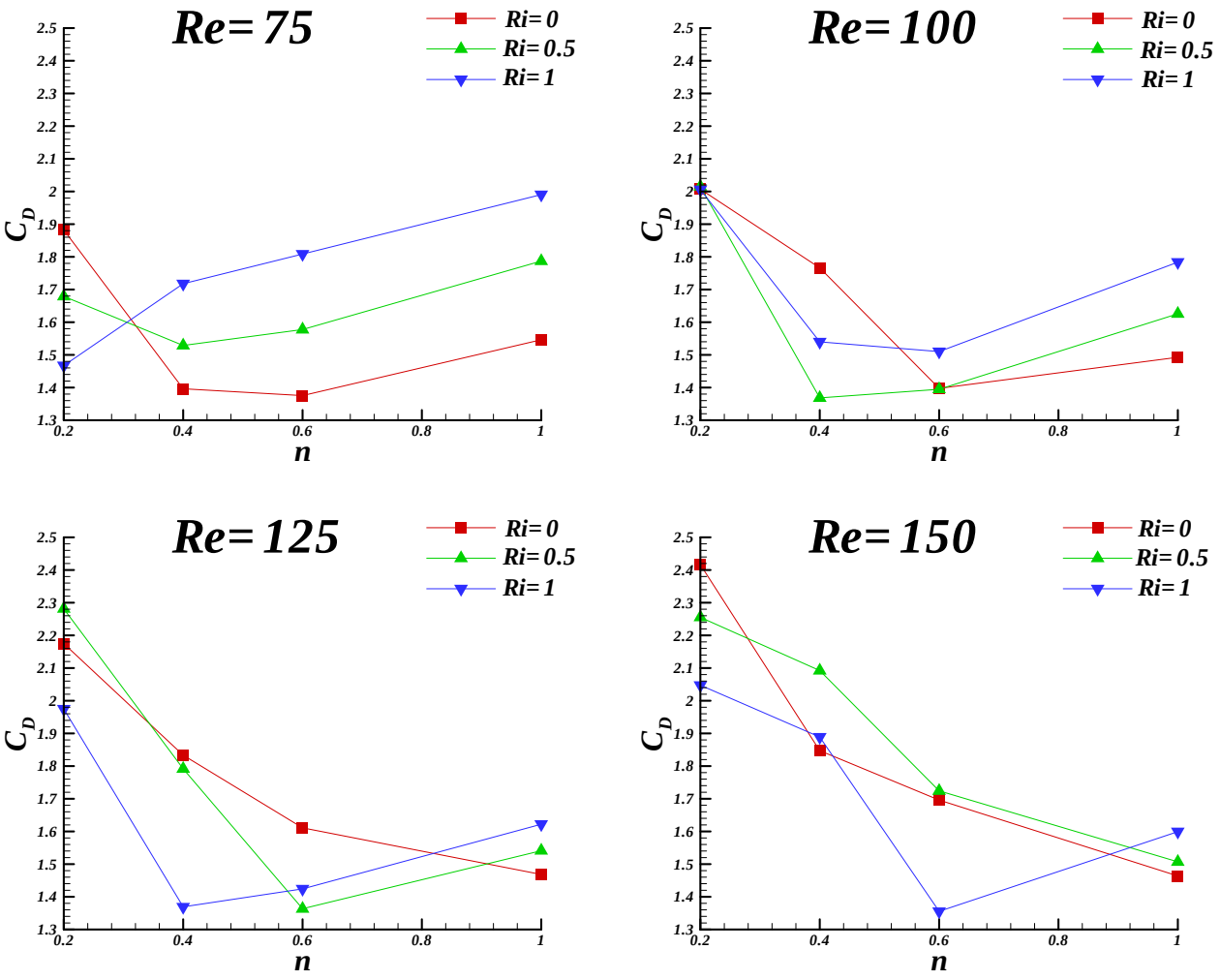

Figure 4.9: *Variation of drag coefficient with power-law index (n)*

It is very much eminent from the above figure (Figure 4.9) that for a constant Re the value of drag coefficients decrease by means of the increased value of n in the shear thinning region

till a certain value after which it increases again. Also, with the increase in the value of Re the drag coefficients record higher values. Initially, the drag coefficient values are the highest for Ri = 0. However, on small increment in the n, there is a cross-over in the curves for unlike Ri thereby emphasizing the fact that the drag coefficient value now enhances with the augment in the aiding buoyancy behavior.

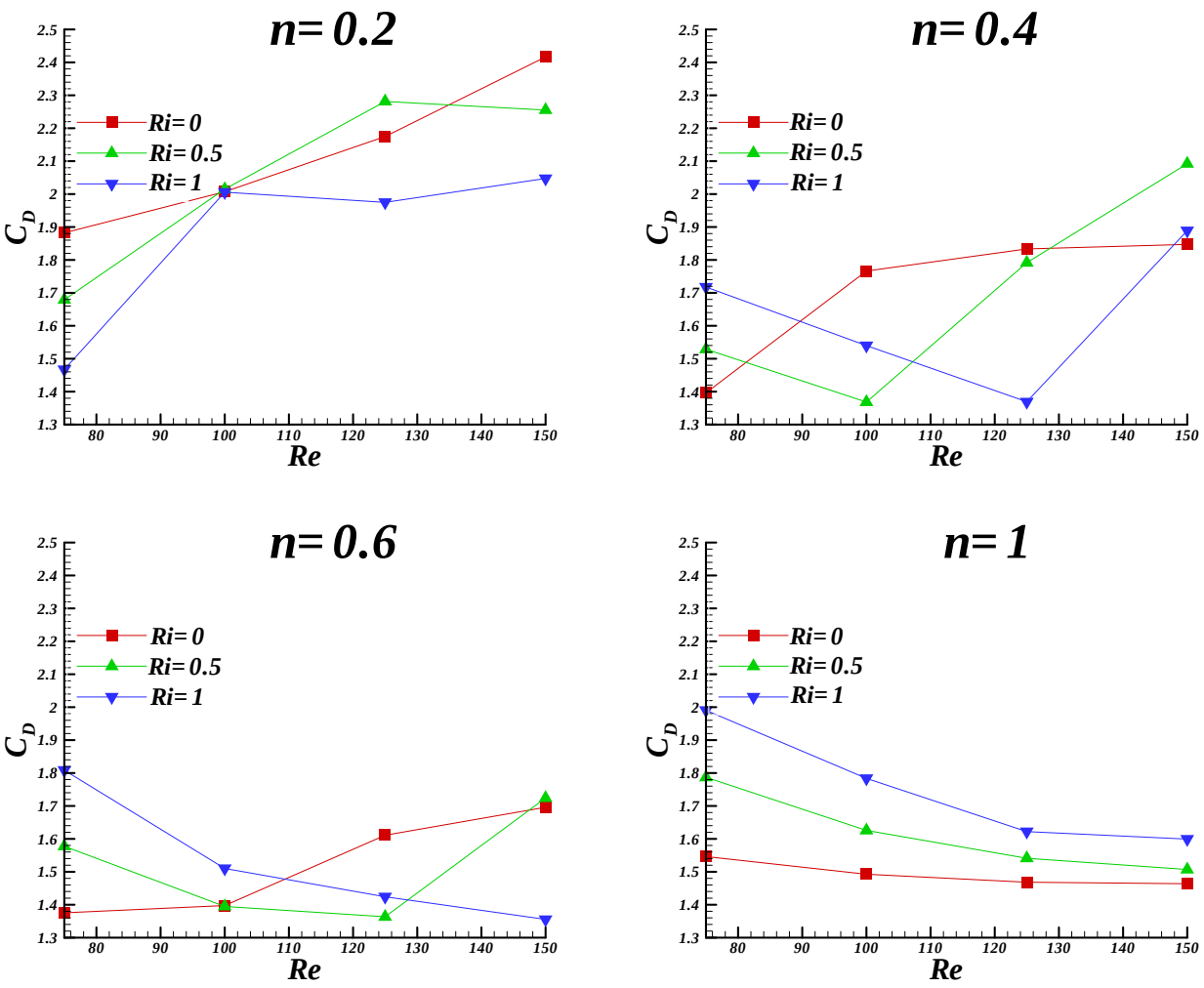

Figure 4.10: *Variation of drag coefficient with Reynolds number (Re) at constant n*

Figure 4.10 suggests that the coefficient of drag reduces with the increment in Re for all values of Ri at n = 1. However, at n = 0.2, the drag coefficients increase with Re for all Ri. At n = 0.4, with the increase in the Re, drag decreases first and then grows for Ri = 0.5 and 1; while the Ri = 1 plot increases monotonically with Re. This anomaly continues to persist at n = 0.6. This nonlinearity in the behavior of drag is consistent with that of Chandra and

Chhabra [26]. On the other hand it can be observed that with increase in the value of n, drag coefficient decreases for a particular value of Ri.

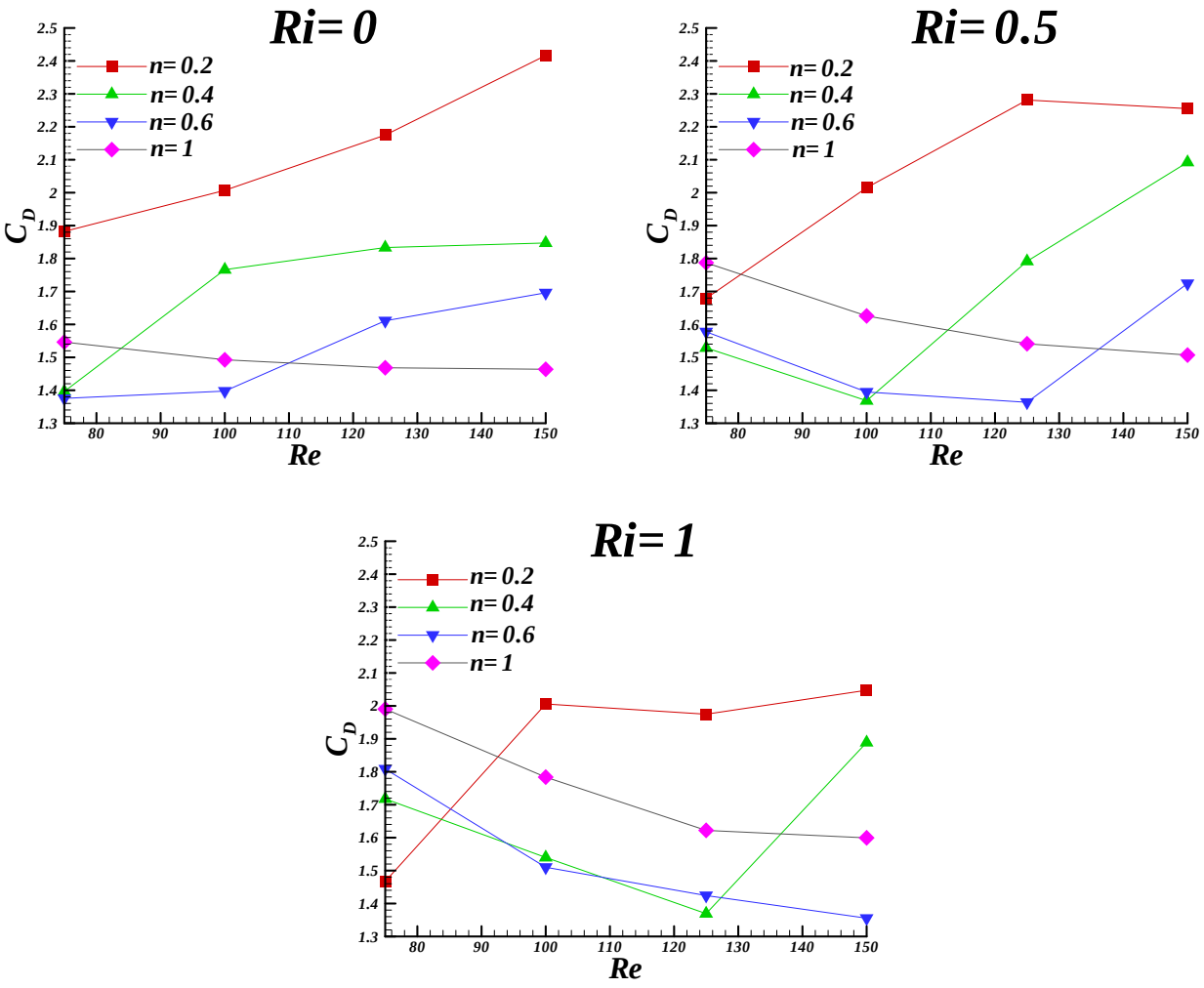

Figure 4.11: *Variation of drag coefficient with Reynolds number (Re) at constant Ri*

It can be stated from Figure 4.11 that drag reduces with the increasing value of n.

4.5. Average Nusselt number (Nu)

To study the heat transfer characteristics of the power-law fluid from the bluff body the dimensionless Nusselt number has been used. For pure forced convection Nu has a behavior such that it rises with rising Re plus pseudo-plastic behavior of fluid. This can be easily explained by the fact that increasing shear-thinning behavior decreases apparent viscosity of the flowing fluid. This reduction in viscosity increases the heat transfer due to less heat dissipation (due to viscosity). Increasing Re clearly indicates increasing flow turbulence.

Mixed convection is seen to increase Nusselt number further than that in forced convection. This effect can be observed to be more prominent at low Re than that at higher Re. Heat transfer increase is seen to be proportional to Reynolds number, Richardson number.

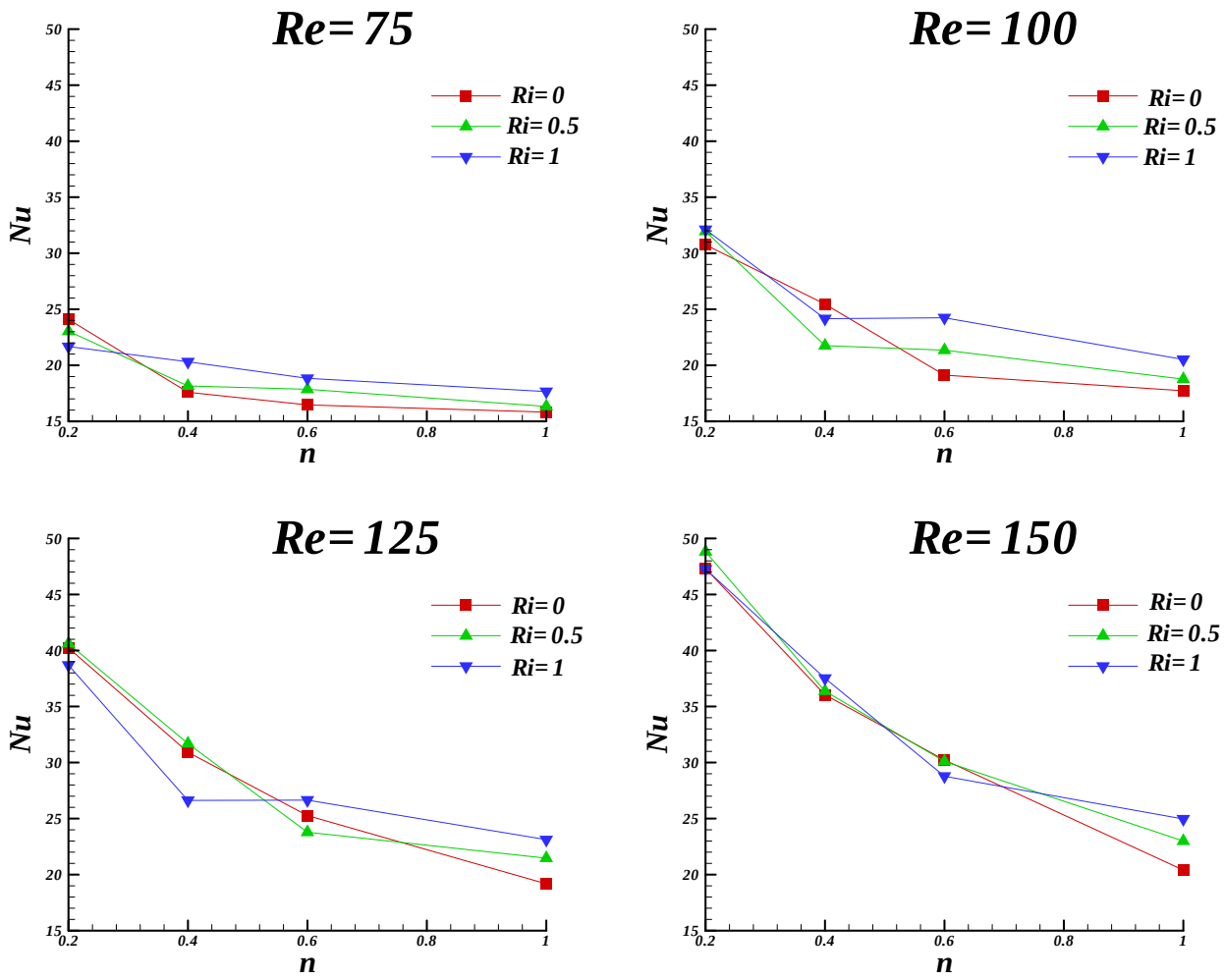

Figure 4.12: *Variation of Nusselt number with power-law index (n)*

This is analyzed from Figure 4.12 that Nu decreases with the raise in the value of n for every Re and Ri. On the contrary, the Nusselt number rises with the rise in the value of Re which is quite evident from Figure 4.12. The relationship between Nusselt numbers with Ri is a bit complex. Initially with rise in the n, Nu is found to be highest for Ri = 0 followed by Ri = 0.5 and 1. However there is a cross-over and eventually Nusselt number for Ri = 1 becomes maximum and that for Ri = 0 becomes minimum. This illustrates the heat transfer parameter in the domain of present study.

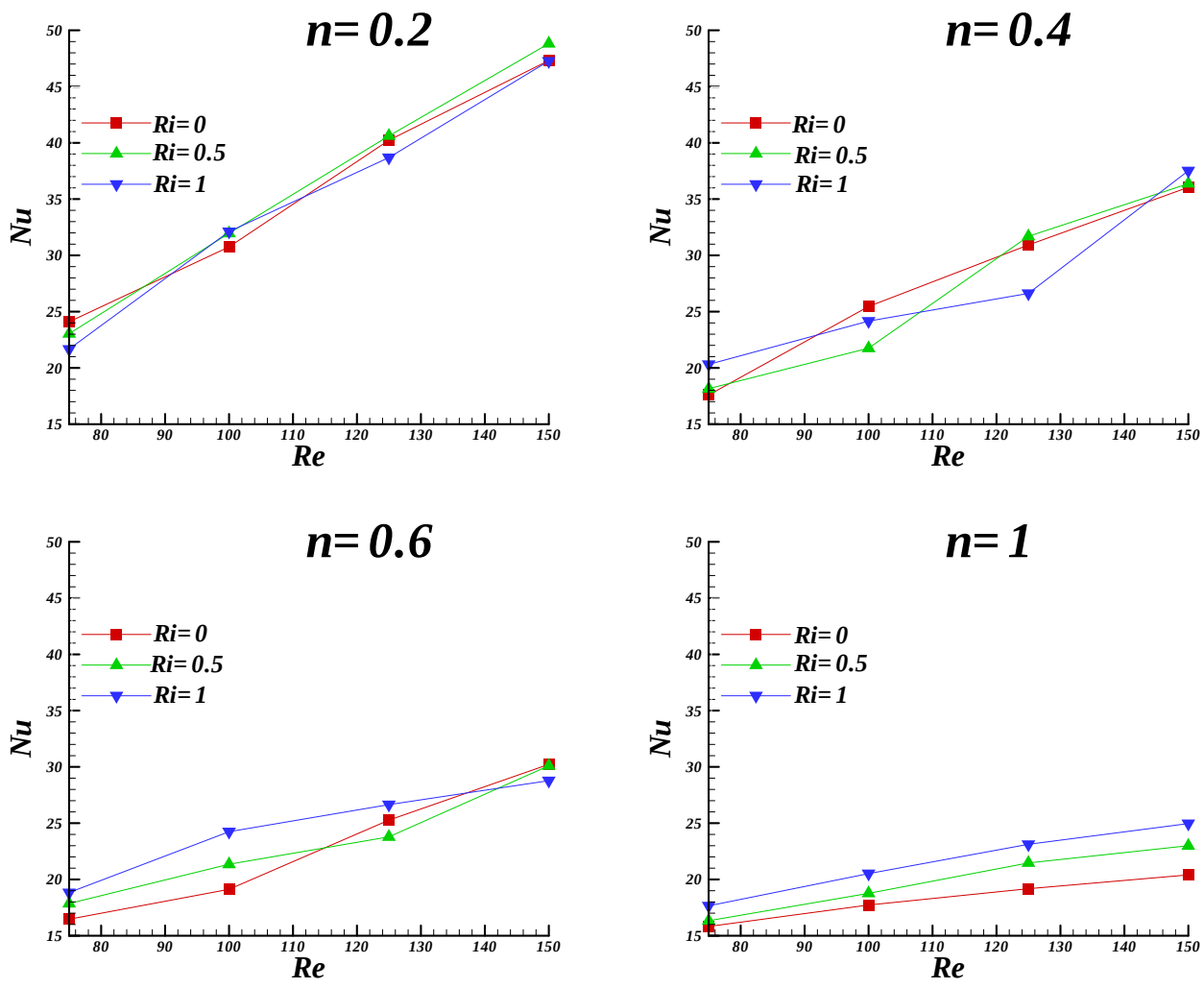

Figure 4.13: *Variation of Nusselt number with Reynolds number (Re) at constant n*

Figure 4.13 suggests that Nu rises with the rise in Re for the entire number of n and Ri. This is clearly attributed to the increase in turbulence with increasing Reynolds number (Re). Furthermore, Nusselt number (Nu) confirms a optimistic dependence on both Re and Pr due to gradual reduction of thermal boundary film with a rise in Reynolds number and Pr. It can be inferred from the above figure that at a particular value of n, increase in Richardson number (Ri) adds to enhancement in heat transfer. This can be securely approved to the information that Richardson number (Ri) is a measure of mixed convection. A positive value of Ri implies mixed convection which obviously has a higher rate of heat transfer as compared to purely forced convection characterized by Ri=0. Thereby, Nu is observed to rise with rising Ri. These results are also consistent with Chandra and Chhabra [26].

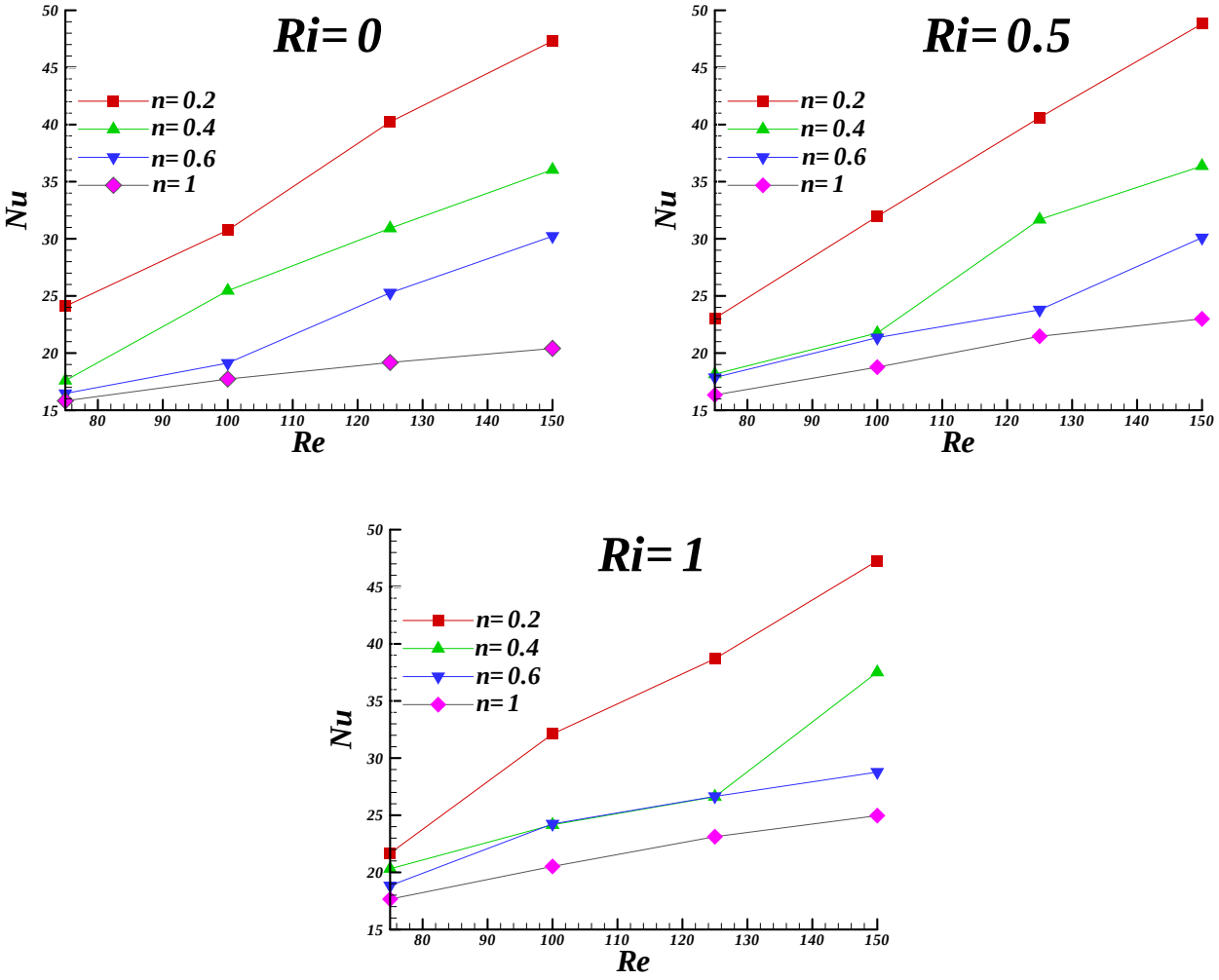

Figure 4.14: *Variation of Nusselt number with Reynolds number (Re) at constant Ri*

All else being same, heat transfer is reported to increase with decreasing value of n as shown in figure 4.14. This draws an explanation from the parameters of effective fluid viscosity and thermal boundary layer. As non-Newtonian flow index (n) decreases, the fluid behavior transmits from Newtonian to pseudo-plastic; this clearly suggests lowering of effective viscosity coupled with thinning of thermal boundary layer.

4.6 Strouhal number (St)

Characterization of fully periodic flow region requires Strouhal number (St) to determine the non-dimensional frequency of vortex shedding. Figure 4.15 explains the deviation of Strouhal number (St) with Re and non-Newtonian flow index (n). As expected, for Newtonian fluids, St increases with Re. With pseudo-plasticity effect periodicity of flow is observed as reported by Chandra and Chhabra [26]. Strouhal number (St) increases as behavior of fluid flow approaches Newtonian from shear thinning at Re=75. As Re further increases St decreases roughly till Re=125 then again rises.

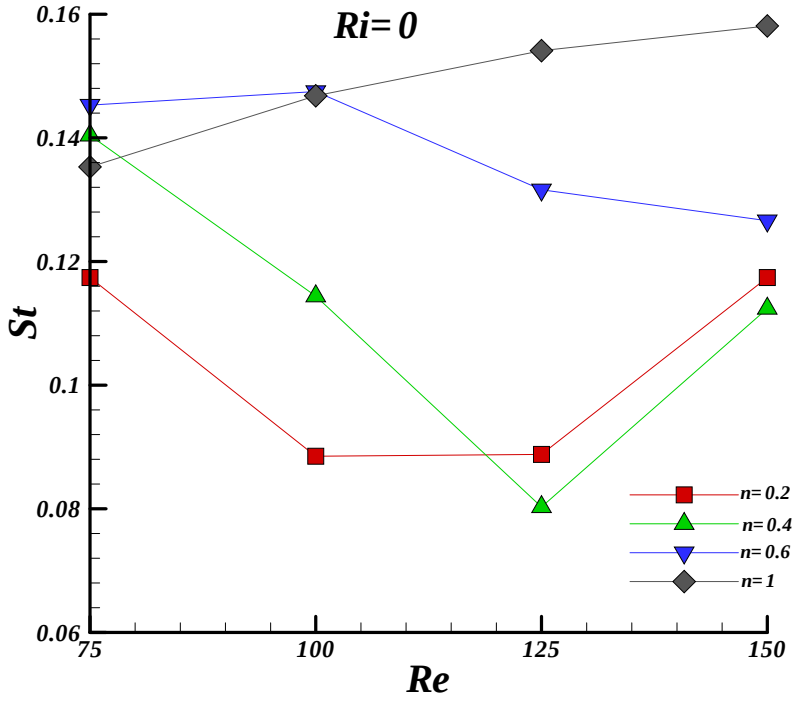

Figure 4.15: *Variation of Strouhal number with Reynolds number (Re) at constant Ri*

CHAPTER - 5

CONCLUSIONS

A numerical study of flow past a heated square cross sectional cylinder in a vertical domain, under the influence of aiding buoyancy has been reported. The ranges of the engineering parameters are: Reynolds number (Re) $75 \leq Re \leq 150$, Richardson number (Ri) $0 \leq Ri \leq 1$ (forced and mixed convection), n = 0.2 to 1 at a constant Prandtl number (Pr) = 50. As predictable, for fluids having $n < 1$, the impact of Re, Pr, and non-Newtonian flow index on fluid flow and thermal exchange behaviors is observed to be more complex than that on the Newtonian fluids. For the Newtonian fluids, at lower Re the isotherms are found to be spread out as viscous forces are dominant while enhancement in heat transfer at higher Re has been confirmed by closely spaced isotherms for a fixed value of Ri and Pr. The isotherms are found to cluster highest at the front, then at right and left and are least close at rear portion of the bluff body which clearly implies that the thermal exchange rate is highest on the front face of the square cylinder and least at the rear portion. The total drag (C_D) is found to decrease with increase in Re at fixed value of Ri. However, Nusselt number shows opposite behaviour, as expected. Alternatively, for shear-thinning fluids, the maximum local Nusselt number may occur at some intermediate location, similar to the observation of a semi-circular cylinder immersed in power-law fluids [26]. Due to lower effective viscosity, shear-thinning fluid behavior enhances the rate of heat transfer which is further aided by higher Reynolds number. Mixed convection (characterized by $Ri>0$) is seen to increase Nusselt number further than that in forced convection. As theory suggests, Strouhal number increases with Reynolds number (Re) for Newtonian fluids. While for shear thinning fluid behavior, periodicity of flow is observed. Strouhal number is found to reduce roughly till Re=125 then again rises.

References

[1] H.M. Badr, Laminar combined convection from a horizontal cylinder-parallel and contra flow regimes, Int. J. Heat Mass Transfer 27 (1984) 15-27.

[2] G. Gandikota, S. Amiroudine, D. Chatterjee and G.Biswas, The effect of aiding/opposing buoyancy on two-dimensional laminar flow across a circular cylinder, Num. Heat Transfer, Part A 58 (2010) 385-402.

[3] A.T. Srinivas, R.P. Bharti, R.P. Chhabra, Mixed convection heat transfer from a cylinder in power-law fluids: Effect of aiding buoyancy, Ind. Eng. Chem. Res. 48(2009) 9735-9754.

[4] A. Okajima, Numerical simulation of flow around rectangular cylinders, J. Wind Eng. Ind. Aerodyn. 33 (1990) 171-180.

[5] K. Nakabe, H. Hasegawa, K. Matsubara, K. Suzuki, Heat transfer from a heated cylinder in a flow between parallel plates in a free-forced combined convection regime, Proceedings, 9th Int. Symp. on Trans. Phen. in Them. Fluids Eng., Singapore (1996) 651-656.

[6] T. Tamura, T. Miyagi, T. Kitagishi, Numerical prediction of unsteady pressures on a square cylinder with various corner shapes, J. Wind Eng. and Indus. Aerodyna. 74-76 (1998) 531-542.

[7] B.A/K. Abu-Hijleh, Laminar mixed convection correlations for an isothermal cylinder in cross flow at different angles of attack, Int. J. Heat Mass Transfer 42 (1999) 1383-1388.

[8] S. Turki, H. Abbassi, S.B. Nasrallah, Two-dimensional laminar fluid flow and heat transfer in a channel with a built-in square cylinder, Int. J. Them. Sci. 42 (2003) 1105-1113.

[9] A. Sharma, V. Eswaran, Effect of aiding and opposing buoyancy on the heat and fluid flow across a square cylinder at Re = 100, Num. Heat Transfer, Part A 45 (2004) 601-624.

[10] A. Sharma, V. Eswaran, Effect of channel-confinement and aiding/opposing buoyancy on the two-dimensional laminar flow and heat transfer across a square cylinder, Int. J. Heat Mass Transfer 48 (2005) 5310-5322.

[11] B. Paliwal, A. Sharma, R.P. Chhabra, V. Eswaran, Power-law fluid flow past a square cylinder: momentum and heat transfer characteristics, Chem. Eng. Sci. 58 (2003) 5315-5329.

[12] A.K. Dhiman, R.P. Chhabra, V. Eswaran, Steady flow of power-law fluids across a square cylinder, Chem. Eng. Res. Des. 84 (2006) 300-310.

[13] A.K. Dhiman, R.P. Chhabra, V. Eswaran, Flow and heat transfer across a confined square cylinder in the steady flow regime: Effect of Peclet number, Int. J. of Heat Mass Transfer 48 (2005) 4598-4614.

[14] S.K. Singh, P.K. Panigrahi, K. Murlidhar, Effect of buoyancy on the wakes of circular and square cylinders: aschlieren-interferometric study, Exp. Fluids 43 (2007) 101-123.

[15] A.K. Dhiman, R.P. Chhabra, V. Eswaran, Steady mixed convection across a confined square cylinder, Int. Comm. Heat Mass Transfer, 35 (2008) 47-55.

[16] G. Biswas, S. Sarkar, Effect of thermal buoyancy on vortex shedding past a circular cylinder in cross-flow at low Reynolds numbers, Int. J. Heat Mass Transfer 52 (2009) 1897-1912.

[17] S.B. Paramane, A. Sharma, Effect of cross-stream buoyancy and rotation on the free-stream flow and heat transfer across a cylinder, Int. J. Them. Sci. 49 (2010) 2008-2025.

[18] S. Sarkar, A. Dalal, G. Biswas, Mixed convective heat transfer from two identical square cylinders in cross flow at Re = 100, Int. J. Heat Mass Transfer 53 (2010) 2628-2642.

[19] P. Koteswara Rao, A.K. Sahu, R.P. Chhabra, Momentum and heat transfer from a square cylinder in power-law fluids, Int. J. Heat Mass Transfer 54 (2011) 390-403.

[20] A.K. Dhiman, N. Sharma, S. Kumar, Wall effects on the cross-buoyancy Around a square cylinder in the steady regime, Brazilian J. Chem. Eng. 29 (2012) 253-264.

[21] D. Chatterjee, B. Mondal, Effect of thermal buoyancy on vortex shedding behind a square cylinder in cross flow a low Reynolds numbers, Int. J. Heat Mass Transfer 54 (2011) 5262-5274.

[22] C. Sasmal, R.P. Chhabra, Effect of orientation on laminar natural convection from a heated square cylinder in power-law liquids, Int. J. Them. Sci. 57 (2012) 112-125.

[23] N. Sharma, A.K. Dhiman, S. Kumar, Mixed convection flow and heat transfer across a square cylinder under the influence of aiding buoyancy at low Reynolds numbers, Int. J. Heat Mass Transfer 55 (2012) 2601-2614.

[24] A.K. Dhiman, N. Anjaiah, R.P. Chhabra, V. Eswaran, Mixed convection from a heated square cylinder to Newtonian and power-law fluids, Trans. ASME J. Fluids Eng. 129 (2007) 506-513.

[25] A.K. Sahu, R.P. Chhabra, V. Eswaran, Two-dimensional unsteady laminar flow of a power-law fluid across a square cylinder, J. Non-Newtonian Fluid Mechanics 160 (2009) 157-167.

[26] A. Chandra, R. P. Chhabra, Momentum and heat transfer from a semi-circular cylinder to power law fluids in vortex shedding regime, Num. Heat Transfer, Part A 63 (2013) 489-510.

[27] www.physics.iitm.ac.in/~compflu/Lect-notes/chhabra.pdf.

Publication

[1] A. K. Dhiman, Shishir Gupta, Laminar mixed convection around a vertical square cylinder, conference, 4th International congress on computational mechanics and simulation (ICCMS), IIT Hyderabad (2012).